JCI The Journal of Clinical Investigation

Residual endotoxin induces primary graft dysfunction through ischemia-reperfusion-primed alveolar macrophages

Mahzad Akbarpour, … , G.R. Scott Budinger, Ankit Bharat

J Clin Invest. 2020. https://doi.org/10.1172/JCI135838.

Research In-Press Preview Immunology Transplantation

Graphical abstract

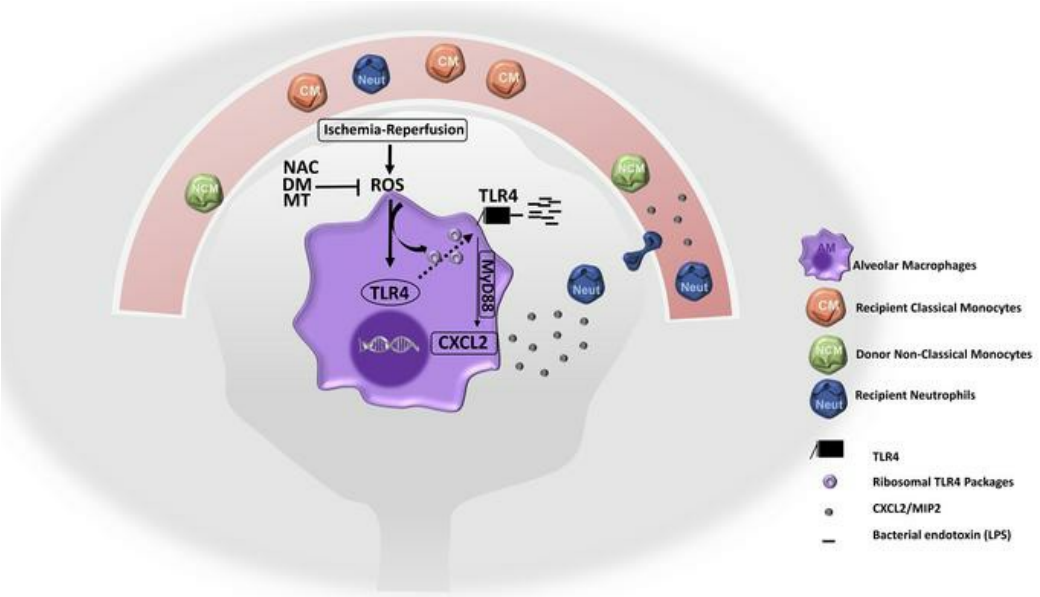

Find the latest version:

https://jci.me/135838/pdf

Residual endotoxin induces primary graft dysfunction through ischemia-reperfusion-primed alveolar macrophages

Mahzad Akbarpour[1], Emilia Lecuona[1], Stephen F. Chiu[1], Qiang Wu[1], Melissa Querrey[1], Ramiro Fernandez[1], Félix L. Núñez-Santana[1], Haiying Sun[1], Sowmya Ravi[1], Chitaru Kurihara[1], James M. Walter[2], Nikita Joshi[2], Ziyou Ren[2], Scott C. Roberts[3], Alan Hauser[2,3], Daniel Kreisel[4,5], Wenjun Li[4], Navdeep S. Chandel[2], Alexander V. Misharin[2], Thalachallour Mohanakumar[5], G. R. Scott Budinger[2], Ankit Bharat[1,2].

[1]Division of Thoracic Surgery, [2]Division of Pulmonary and critical Care Medicine and [3]Department of Microbiology-Immunology, Feinberg School of Medicine, Northwestern University, Chicago, IL, USA.

[4]Department of Surgery and [5]Department of Pathology and Immunology, Washington University in St. Louis, St. Louis, MO, USA.

[5]Norton Thoracic Institute, St. Joseph's Hospital and Medical Center, Phoenix, AZ

Corresponding author:

Ankit Bharat, MD, FACS

Northwestern University Feinberg School of Medicine.

Divisions of Thoracic Surgery, Pulmonary and Critical Care Medicine

676 N. Saint Clair Str, Ste 650

Chicago, IL, 60611.

Tel: 312-926-7552

abharat@nm.org

Conflict of interest: The authors have declared that no conflict of interest exists.

Abstract

Despite the widespread use of antibiotics, bacterial pneumonias in donors strongly predispose to the fatal syndrome of primary graft dysfunction (PGD) following lung transplantation. We report that bacterial endotoxin persists in human donor lungs after pathogen is cleared with antibiotics and is associated with neutrophil infiltration and PGD. In mouse models, depletion of tissue-resident alveolar macrophages (TRAM) attenuated neutrophil recruitment in response to endotoxin as shown by compartmental staining and intravital imaging. Bone marrow chimeric mice revealed that neutrophils were recruited by TRAM through activation of TLR4 in a MyD88-dependent manner. Intriguingly, low levels of endotoxin, insufficient to cause donor lung injury, promoted TRAM-dependent production of CXCL2, increased neutrophil recruitment, and led to PGD, which was independent of donor non-classical monocytes. Reactive oxygen species (ROS) increased in human donor lungs starting from the warm-ischemia phase and were associated with increased transcription and translocation to the plasma membrane of TLR4 in donor TRAM. Consistently, scavenging ROS or inhibiting their production to prevent TLR4 transcription/translocation or blockade of TLR4 or co-receptor CD14 on donor TRAM prevented neutrophil recruitment in response to endotoxin and ameliorated PGD. Our studies demonstrate that residual endotoxin after successful treatment of donor bacterial pneumonia promotes PGD through ischemia-reperfusion-primed donor TRAM.

Introduction

Prolonged mechanical ventilation, aspiration of gastric contents into the lungs around the time of death, and immune dysfunction after brain death all contribute to increased rates of bacterial infections in donor lungs (1, 2). Despite the routine use of bronchoalveolar lavage culture and empiric and pathogen-directed antimicrobial therapy, the presence of bacteria in donor lungs is associated with increased risk for primary graft dysfunction (PGD), the predominant cause of mortality following lung transplantation (3). These high rates of bacterial recovery and the associated PGD following transplant are major reasons why donor lungs have a utilization rate of only about 15%, which is one of the lowest amongst all solid organs (www.unos.org). The low utilization of donor lungs accounts for the high mortality and long wait times observed in patients requiring lung transplantation. How bacteria in the donor lungs predispose to the pathogenesis of PGD and why antimicrobial therapy is unable to prevent lung allograft injury remains unclear.

Host neutrophils recruited to the lung allograft mediate lung ischemia-reperfusion injury leading to PGD, the most important risk factor for early and chronic allograft failure, but are also necessary for the clearance of bacterial and fungal pathogens (4-13). Since neutrophil depletion is unlikely to be tolerated in immunosuppressed lung transplant patients, it is critical to delineate mechanisms leading to neutrophil recruitment immediately after transplant. The severity of neutrophil recruitment and the resulting PGD varies dramatically between lung transplant recipients. Because broad-spectrum antibiotics targeting most gram-negative organisms are routinely administered to both the donor and recipient before transplant, the role of bacteria in the donor lung in driving this heterogeneity has been overlooked.

Surprisingly, we detected lipopolysaccharide, also referred to as endotoxin, in human donor lungs with bacterial pathogens prior to transplant, despite antibiotic therapy. Lipopolysaccharide (LPS)

is a prototypical pathogen-associated molecular pattern (PAMP) in the outer cytoplasmic membrane of gram-negative bacteria which signals through TLR4 receptors to induce neutrophil influx into the alveolar space (4, 14). We recently discovered that donor origin pulmonary intravascular non-classical monocytes (NCM) trigger neutrophil recruitment following lung transplantation through the production of neutrophil chemoattractant CXCL2 (11, 13, 15). The donor NCM also recruit spleen-derived $CCR2^{+}$ classical monocytes (CM) to the allograft, which contribute to neutrophil extravasation, worsening lung injury (12). Thus, both donor derived NCM and recipient CM play complementary roles in neutrophil recruitment and extravasation to initiate lung transplant ischemia-reperfusion injury. These mechanisms differ from observations in naïve mice treated with LPS in which tissue resident alveolar macrophages (TRAM), or other cell populations in the lung, may be necessary for neutrophil recruitment (16-19). We, therefore, hypothesized that LPS from the different bacterial pathogens, and perhaps other PAMPs, persisting after successful antimicrobial therapy, contribute to excessive neutrophil recruitment after lung transplantation by augmenting signaling through NCM or CM, and/or activated parallel pathways through TRAM.

We found that endotoxin can persist in human donor lungs despite pathogen clearance and is associated with increased neutrophil infiltration and PGD after lung transplantation. Pharmacologic and genetic depletion of donor NCM attenuated neutrophil recruitment following transplant of naive donor lungs (12, 13), but did not abrogate neutrophil recruitment and PGD in donor lungs containing endotoxin. In addition, exposure of donor TRAM to ischemia-reperfusion primed them to release CXCL2 in response to endotoxin through a TLR4/MyD88 pathway, obviating the requirement for donor NCM in neutrophil recruitment to the allograft. Donor lungs produced reactive oxygen species (ROS), beginning in the warm-ischemia phase, which led to both an increase in TLR4 transcription and its translocation to the cell plasma membrane.

Accordingly, ROS scavengers, blockade of TLR4, or TLR4 co-receptor CD14, resulted in amelioration of PGD when endotoxin was present in the donor lungs. Our results suggest that a multipronged strategy that targets both TRAM and non-classical monocytes within the donor lung can reduce the severity of PGD in donors with a history of bacterial pneumonia or colonization.

Results

Endotoxin persists in donor lung despite pathogen clearance and predisposes to primary graft dysfunction (PGD). Recruitment of host neutrophils to the lung allograft following lung transplantation mediates lung ischemia-reperfusion injury (10). To determine whether bacterial split products in the donor lung could exacerbate neutrophil influx after transplant, we analyzed human donor lungs that were positive for gram-negative bacteria prior to transplant but treated with antimicrobials. These human donor lungs had normal P:F ratio in the donor prior to transplant and no pulmonary infiltrates on chest radiograph or computed tomography. Successful treatment of the infection was evident by negative microbial cultures of bronchoalveolar fluid (BALF) collected at the time of transplantation. However, as shown in Figure 1A, the BALF of successfully treated human donor lungs obtained at transplant revealed residual endotoxin which persisted following transplantation. Intriguingly, following transplantation, these endotoxin containing donor lungs showed physiological markers of injury including significantly higher neutrophil infiltration as well as reduced P:F ratio post-transplant, compared to those without endotoxin (Figures 1B and 1C), although there was no significant difference in the neutrophil count and P:F ratio between the two groups in the donor prior to lung procurement (Figure 1B and 1C). We replicated these observations in a murine model of lung transplantation by administering intra-tracheal (IT) PBS control or low dose of LPS from three different bacteria (0.5 µg/g BW *E.coli,* 0.2 µg/g BW *P. aeruginosa* or 0.2 µg/g BW *K. pneumoniae*) to donor mice prior to transplantation into allogeneic murine recipients. The low dose was insufficient to cause neutrophil infiltration or injury in the

native lungs. However, the grafts containing LPS experienced severe PGD at 24 h, which was associated with increase in chemokines in the BALF (Supplemental Figure 1) including CXCL2, a potent neutrophil chemoattractant (13, 20), as well as profound neutrophil influx (Figure 1D). These data suggested that low levels of endotoxin may not cause clinically significant lung injury; however, following ischemia-reperfusion, the susceptibility of lung allografts to residual endotoxin increases significantly. Finally, recent studies have suggested that donor microbiome may play a role in the development of lung allograft rejection (21-24). Since the role of donor lung microbiome in the pathogenesis of PGD is uncertain, we analyzed the BALF from human donor lungs by 16S PCR high-throughput screening, as described before (25, 26). BAL samples were distinct from rectal samples ($R = 0.977$, $p = 0.002$), and no microbial clustering within BAL samples was apparent. PGD sample (patient 9) was not dissimilar from non-PGD samples (patient 1-7, 8, 10) ($R = -0.279$, $p = 0.625$). There was also no variation in the donor lung microbiome with regards of endotoxin containing organisms and, therefore, less likely to directly explain our results (Supplemental Figure 2).

CXCL2 secreted from tissue resident alveolar macrophages (TRAM) contributes to neutrophil recruitment and lung injury following bacterial infection or LPS administration.

To determine the mechanisms by which endotoxin in donor lungs accentuates PGD, we first studied the mechanism of endotoxin induced lung injury in the native mouse lung. Given that LPS from all three bacterial species induced PGD and neutrophil influx, for subsequent studies, we used LPS from *E.coli* since it has been used most commonly in published literature. Consistent with prior reports, we found that 24 h after high dose (2 µg/g BW) IT LPS administration there was a robust neutrophil influx (Supplemental Figure 3A) in native lungs with more than 80% of neutrophil extravasated into the alveolar space (Supplemental Figure 3B). This was accompanied by pulmonary edema and histologic signs of injury (Supplemental Figure 3C and 3D) (27, 28). We

then performed RNASeq analysis of flow-sorted TRAM isolated from BALF in patients with severe pneumonia resulting in respiratory failure in our medical intensive care unit (16). Specifically, we compared alveolar macrophage transcriptomes from patients with confirmed pneumonia secondary to *Pseudomonas aeruginosa* (based on quantitative culture of the same BALF sample) to transcriptomes of patients with negative quantitative culture and found that differentially expressed genes were associated with GO processes involved in immune activation (Figure 2A and 2B). We found that those genes associated with the GO processes in human subjects were also differentially expressed in the TRAM of humanized MISTRG mouse infected with *Pseudomonas* (Figure 2C). Furthermore, compared to those without pneumonia, TRAM from patients with *Pseudomonas* pneumonia and MISTRG mice infected with *P. aeruginosa* demonstrated a significant increase in the expression of the primary neutrophil chemokine, CXCL2 (Figure 2D), which we have shown to be pivotal in neutrophil chemotaxis to the re-perfused lung allograft (11, 13, 15).

To further investigate whether TRAM were responsible for CXCL2 production in response to LPS in TLR4-dependent manner, we analyzed expression of *TLR4* in previously published single cell RNA-seq datasets generated from non-diseased human lungs (29,30, 31) (Supplemental Figure 4). Expression of *TLR4* was largely restricted to *FABP4*-positive TRAM, although some endothelial cells and monocytes also demonstrated expression of *TLR4*. Given that endothelial cells face the vasculature and monocytes in human lungs are largely retained in the blood vessels (13, 32), TRAM are likely to be the predominant secretors of CXCL2 in response to TLR4 stimulation by LPS present in the alveolar space. Nevertheless, to confirm that TRAM drive neutrophil recruitment in response to LPS, we administered clodronate-loaded liposomes intratracheally to selectively deplete TRAM in wild-type (WT) mice (Supplemental Figure 5). Depletion of TRAM prior to LPS challenge in WT mice resulted in a significant decrease in CXCL2

levels in BALF (Figure 3A) along with a significant reduction in neutrophil infiltration in lung tissue, determined by flow cytometry (Figure 3B) and two-photon microscopy (Figure 3C and 3D. Supplemental Video 1 and 2). Next, to determine whether CXCL2 signaling was necessary for neutrophil recruitment in response to LPS, we treated mice with anti-CXCL2 antibodies (13). Neutralization of CXCL2 resulted in a significant attenuation of neutrophil recruitment to the injured lungs, 24 h after LPS administration (Figure 3E). Similarly, mice deficient in the CXCL2 receptor (*Cxcr2*$^{-/-}$) did not develop neutrophil influx in response to IT LPS (Figure 3F). Moreover, depletion of circulating classical monocytes (CM) using anti-CCR2 antibody (Supplemental Figure 6A, 6B and 6C), non-classical monocytes (NCM) using intravenously administered Clo-lip (Supplemental Figure 6D, 6E and 6F), or simultaneous depletion of monocytes, peribronchial interstitial macrophages and lung CD11b+ dendritic cells, using CD11b-DTR system, had no effect on neutrophil trafficking in response to IT LPS (Supplemental Figure 6G and 6H). Taken together, these data demonstrate that TRAM are responsible for neutrophil influx in response to LPS through the production of CXCL2.

Donor TRAM exacerbate PGD in donor lung containing endotoxin through the production of CXCL2. We have recently shown that donor origin pulmonary intravascular NCM recruit neutrophils following transplant and contribute to the pathogenesis of PGD in a mouse model of lung transplantation (12, 13). As bacterial infections are common in human donor lungs, we investigated whether NCM, TRAM, or both, would mediate neutrophil recruitment in donor lungs exposed to LPS. Accordingly, we treated donors with a low-dose of LPS (0.5 µg/g BW), insufficient to cause donor lung injury, and found that while LPS-free donor lungs from mice lacking NCM (*Nr4a1*$^{-/-}$) did not develop neutrophil recruitment and PGD following lung transplantation (13), in contrast, donor lungs from low-dose LPS-treated *Nr4a1*$^{-/-}$ mice did (Figure 4A and 4B). Similarly, pharmacological depletion of donor NCM using IV Clo-lip prevented neutrophil recruitment

following murine lung transplant of LPS-free (13), but not of LPS-containing donor lungs (Figure 4A and 4B), suggesting that neutrophil recruitment associated with LPS in donor lungs is NCM independent. On the other hand, depletion of TRAM in LPS-treated *Nr4a1*$^{-/-}$ donor lungs prior to transplant using IT Clo-lip or depletion of both TRAM and NCM by IT plus IV Clo-lip in WT donor lungs attenuated the LPS-induced neutrophil infiltration (Figure 4A and 4B).

We have reported that *Nr4a1*$^{-/-}$ donor lungs have reduced CXCL2 levels following transplant when compared with WT donor lungs (13). However, administration of low-dose LPS to *Nr4a1*$^{-/-}$ donor lungs before transplantation resulted in increased CXCL2 levels (Figure 4C). We also found increased CXCL2 mRNA expression in TRAM isolated from human donor lungs positive for endotoxin compared to those negative for endotoxin following transplantation reperfusion (Figure 4D). To determine whether CXCL2 was necessary for the recruitment of neutrophils in endotoxin containing donor lungs, we treated recipients with an anti-CXCL2 antibody immediately after transplantation or used *Cxcr2*$^{-/-}$ mice as transplant recipients. In both cases, neutrophil recruitment after transplantation of the endotoxin-containing donor lung was attenuated (Figure 4A and 4B). Collectively, these result show that ischemia-reperfusion primed TRAM can recruit neutrophils in lung allografts containing low levels of endotoxin through CXCL2 release, obviating the requirement for NCM.

TRAM-mediated neutrophil recruitment in response to endotoxin is dependent on TLR4-MyD88 signaling. The pattern recognition receptor for LPS is toll-receptor 4 (TLR4), which interacts with the intracellular adaptor protein MyD88 to enable signal transduction (33). In order to test whether the TLR4-MyD88 signaling pathway was responsible for the LPS-priming of TRAM prior to lung transplantation, we crossed *Cd11c*^{Cre} transgenic mice with *Myd88*$^{flox/flox}$ (*Myd88*$^{\Delta}$) mice to generate *Cd11c*^{Cre}*Myd88*$^{\Delta}$ mice, which lack MyD88 expression specifically in TRAM and DC.

Cd11c^{Cre}*Myd88*$^{\Delta}$ mice had similar numbers of TRAM compared to WT mice (Figure 5A); however, they showed an attenuated neutrophil infiltration to the lungs in response to LPS (Figure 5B). We then performed a rescue experiment in which we treated the *Cd11c*^{Cre}*-Myd88*$^{\Delta}$ mice with IT liposomal clodronate to deplete TRAM lacking MyD88 expression, and then adoptively transferred TRAM from WT or *Tlr4*$^{-/-}$ mice. As shown in Figures 5C and 5D, reconstitution with WT TRAM restored neutrophil infiltration, while reconstitution with TRAM lacking TLR4 expression showed no difference in neutrophil recruitment compared to *Cd11c*^{Cre}*Myd88*$^{\Delta}$ mice. This indicated that the neutrophil recruitment by TRAM in response to LPS is dependent on TLR4-MyD88 signaling.

Lung transplant ischemia-reperfusion activates TRAM to increase CXCL2 production in response to endotoxin via TLR4 regulation. Human TRAM isolated from donor lungs containing endotoxin produced increased amounts of CXCL2 following reperfusion compared to TRAM isolated from endotoxin-free human lungs (Figure 6A). Moreover, ischemia-reperfusion primed human donor TRAM produced more CXCL2 *in vitro* in response to the same amount of endotoxin compared to their native state (Figure 6B and Supplemental Figure 7). Therefore, we explored the role of ischemia-reperfusion in priming TRAM to endotoxin using murine models. Similar to humans, TRAM isolated from murine donor lungs post-ischemia produced significantly more CXCL2 upon stimulation with LPS (Figures 6C and 6D). We next performed RNAseq analysis of donor TRAM experiencing ischemia-reperfusion injury (13, 34), which revealed upregulation of TLR4 and its co-receptor CD14 (Figure 7A). We validated these findings by performing quantitative real-time PCR of TRAM isolated from murine donor lungs pre- and post-ischemia (Figure 7B). To understand TLR4 regulation during ischemia-reperfusion injury, we performed a time course during post-ischemia, analyzing both *Tlr4* mRNA levels and protein expression at the plasma membrane in TRAM. We found that *Tlr4* mRNA levels started increasing 4 h post-ischemia, reaching significance at 24 h (Figure 7C). Using flow cytometry, we determined

that TLR4 protein expression at the plasma membrane reached statistical significance at 4 h post-ischemia keeping a constant expression at 24 h (Figure 7D). Moreover, immunocytochemistry (ICC) performed in donor TRAM isolated at serial time points following transplantation showed that TLR4 increasingly accumulated towards the cell periphery following transplantation (Figure 7E, Supplemental Figure 8 and Supplemental Figure 9). These results suggest that ischemia-reperfusion injury induces TLR4 translocation to the plasma membrane at earlier time points (35) followed by increased *de novo* synthesis at later time points. Finally, to determine whether TLR4 signaling is necessary for LPS-induced activation of donor lung TRAM, we administered LPS in the presence of TLR4 antagonist (TAK-242) or CD14/TLR4 antagonist (IAXO-101) and then transplanted these lungs into WT recipients. We found that anti-TLR4 treatment suppressed the neutrophil influx post-transplant associated with LPS (Figure 7F).

Reactive oxygen species (ROS) released during warm-ischemia and following reperfusion increase the transcription of TLR4 and its translocation to the cell membrane in TRAM.

ROS generated in the mitochondria have been implicated in signaling pathways activated after ischemia-reperfusion injury (36, 37). To explore whether ROS are necessary for the increased transcription of *TLR4* in donor TRAM, we analyzed ROS generation in donor human lung tissue and *TLR4* mRNA expression in TRAM at five consecutive time points during ischemia-reperfusion. Donor tissue were harvested at: A) *In situ* native lung: biopsies obtained after opening donor's chest cavity and prior to procurement; B) End of cold-ischemia: biopsies obtained after the donor lung was removed from cold-storage but prior to initiation of implantation; C) End of warm-ischemia: biopsies obtained from the donor lung that sustained warm ischemia during implantation but immediately prior to reperfusion; D) Post-reperfusion 30 min; and E) Post-reperfusion 120 min. We found that ROS increased during the warm-ischemia phase and continued to increase at 30 and 120 min post-reperfusion (Figure 8A). Intriguingly, *TLR4*

transcription in human donor TRAM did not increase until the 30 min post-reperfusion but continued to increase at the 120-min time point (Figure 8A). It was clinically infeasible to evaluate TRAM from the donor lung tissue site at longer time points since the chest of the recipient is closed at the conclusion of the surgical procedure. Accordingly, we performed experiments using exogenous ROS to replicate these findings. We cultured murine TRAM in the presence of 100 μM hydrogen peroxide, as previously described (35). At 1 h, we did not observe any change in *Tlr4* transcription but its translocation to the cell membrane increased significantly (Supplemental Figure 10A and 10B). Unfortunately, we could not evaluate the effects of hydrogen peroxide on TRAM *in vitro* beyond 1 h as we observed progressive cell death at longer time points (Supplemental Figure 10C). Nevertheless, using the murine model of lung transplantation, we could confirm a role for mitochondrial ROS by using the general ROS scavenger N-acetylcysteine (NAC) (38), and the mitochondrial ROS scavengers Mito-Tempo (MT) (39) and dimethyl malonate (DM) (40), to abrogate the ischemia-reperfusion induced increase in *Tlr4* transcription and expression at the plasma membrane. Indeed, donor TRAM did not develop an increase in *Tlr4* transcription or TLR4 protein translocation to the plasma membrane following murine lung transplantation when treated with NAC, MT or DM as demonstrated by both qualitative and quantitative measures (Figures 8B, 8C and 8D). Moreover, NAC treatment prevented neutrophil recruitment and development of PGD in endotoxin containing *Nr4a1*$^{-/-}$ donor lungs (Figures 8E and 8F).

Discussion

Despite the increasing numbers of lung transplants worldwide, there is a significant gap between the demand and availability of lungs for transplants (41). Many potential donor lungs with adequately treated donor pneumonias are turned down at the time of evaluation because of concerns for the development of PGD following transplantation (42-44). While neutrophil

recruitment into the transplanted lung allograft is essential for the development of PGD, a lack of insight into mechanisms that drive neutrophils into the allograft has precluded therapies targeted to the donor or recipient that might attenuate their recruitment and the attendant lung injury. We found that human donor lungs successfully treated for bacterial pneumonia had residual endotoxin despite the clearance of bacterial pathogen. In a mouse lung transplant model, levels of endotoxin insufficient to induce detectable injury in donor lungs was associated with increased neutrophil recruitment as well as physiological markers of allograft injury. This is consistent with the observed association between historic pneumonia in the donor lung and PGD (44).

We used a mouse model of lung transplant to elucidate the mechanisms by which low levels of LPS in the donor lung induces neutrophil recruitment into the allograft. We found that endotoxin in the donor lung primes donor TRAM to release CXCL2 after lung transplantation leading to neutrophil recruitment. We also found that ischemia reperfusion injury upregulates both TLR4 and CD14 on TRAM, potentially creating a feed forward loop to sustain neutrophil recruitment. The importance of LPS/TLR4/MyD88 signaling in TRAM was confirmed by using genetic and pharmacologic inhibitors combined with cell specific depletion and reconstitution studies. In marked contrast to the requirement of NCM for neutrophil recruitment into allografts from naïve donors (13), TRAM in the donor lung were indispensable and NCM were dispensable for neutrophil recruitment in LPS contaminated donors. These findings show that the exposure history in the donor can reshape neutrophil responses during lung transplantation.

Release of ROS during ischemia-reperfusion injury contributes to the pathogenesis of organ dysfunction (37). We analyzed human donor lungs longitudinally to evaluate for the production of ROS. We found that ROS started to increase during the warm ischemia phase and continue to do so following reperfusion, but the increase in TLR4 transcription was not observed until 30 min

following reperfusion (45). As warm ischemia lasts 45-60 minutes, we conclude that the increase in *TLR4* transcription lags generation of ROS by 1-2 h. We confirmed these findings in the murine lung transplant model where the expression of TLR4 increased after transplant and were inhibited using the general ROS scavenger N-acetylcysteine (NAC) (46) as well as the mitochondrial ROS scavengers Mito-Tempo (MT) (39) and dimethyl malonate (DM) (40). Further work is needed to determine the mechanisms by which ROS augment *Tlr4* and *Cd14* transcription and whether ischemia reperfusion driven ROS also augment TLR4 translocation to the plasma membrane via Src-dependent signaling through generation of ceramide as has been described (35, 47).

Our findings provide a mechanistic explanation for the marked and unpredictable heterogeneity between transplant recipients in the incidence and severity of PGD with implications for therapy. Specifically, we found that both primed alveolar macrophages from LPS treated donors and NCM responded to lung transplant mediated ischemia reperfusion injury by releasing CXCL2, also known as MIP-2 (13, 48). While other cytokines and chemokines play a role in the initiation and propagation of the inflammatory response, the focus of our work was on neutrophil recruitment. Our focus on CXCL2 was justified based on our prior publication (13) which revealed a non-redundant role of CXCL2 in neutrophil recruitment to the allograft following lung transplantation and supported by our analysis of several other cytokines in LPS containing donor lungs (Supplemental Figure 1). Causal evidence comes from the murine transplant model where genetic or pharmacological neutralization of CXCL2 in the LPS primed donor lung reduced neutrophil recruitment. Furthermore, we found that inhibition of mitochondrial ROS, which have been implicated in signaling pathways induced by ischemia reperfusion injury (36, 37), attenuated CXCL2 mediated neutrophil recruitment after lung transplantation. While removing LPS from donor lungs is unlikely to be feasible, treatment of donor lungs with a history of pneumonia with

these inhibitors prior to transplantation might safely reduce the risk of PGD and expand the pool of lungs available for transplantation. Importantly, we were able to confirm key aspects of our murine model in homologous cell populations isolated from patients with severe pneumonia in our intensive care unit and in patients undergoing lung transplantation in our center. More careful phenotyping of the exposure history in the donor lung might reveal additional environmental exposures that drive PGD. Putative exposures can be causally examined in preclinical murine lung transplant models as we show in this study. While our data using bone marrow chimeric mice combined with scRNAseq data implicated TRAM as the predominant cell type necessary for the production of CXCL2, a role for another cell type in the donor lung releasing CXCL2 should be recognized since it has been shown that alveolar epithelial cells can produce CXCL2 in response to pathogens (49). Additionally, while the focus of our study was on neutrophil recruitment that was dependent on CXCL2, it should be emphasized that other cytokines and chemokines would be necessary for the propagation of downstream inflammatory cascade and need to be further elucidated.

Fulminant bacterial infections or high levels of endotoxin will likely lead to severe injury to the donor lungs making them unsuitable for clinical transplantation. Our rationale for using low levels of endotoxin was to specifically test the hypothesis that residual PAMPs which persist after treatment of donor pneumonias and are insufficient to cause injury in the native lungs can drive the pathogenesis of PGD. We recognize that damage-associated molecular patterns (DAMPs), such as HMGB1, might be released during the ischemia-reperfusion phase and trigger TLR4 activation (50, 51). While we tested the role of endotoxin in this study, it is possible that these DAMPs may also contribute to the clinical heterogeneity observed in the incidence of PGD. Hence their role should be explored in future studies. Our current and previously published data suggest the development of PGD involves several cell populations including non-classical monocytes,

neutrophils, alveolar macrophages and classical monocytes. The complex signaling pathways leading to their orchestrated sequential recruitment and activation are incompletely understood. Additionally, whether compartmental separation of these DAMPs and PAMPs can selectively activate donor NCM or TRAM should also be explored. It is intriguing that NCM play a role in neutrophil recruitment in response to DAMPs while recipient classical monocytes permeabilize the pulmonary endothelium to promote neutrophil extravasation (11-13, 15). In contrast, we found that donor TRAM are capable of driving both neutrophil recruitment as well as neutrophil extravasation since depletion of TRAM resulted in significant decrease in both. Whether TRAM mediate neutrophil extravasation through the recruitment of recipient classical monocytes remains unknown. Future studies might examine the role of TRAM in monocyte trafficking to the lung allografts as they might introduce common therapeutic targets to ameliorate both ischemia-reperfusion and endotoxin-associated lung allograft injury.

Our study suggests several avenues for future investigation. While the data using bone marrow chimeric mice combined with scRNAseq data implicated TRAM as the predominant cell type necessary for the production of CXCL2, it has been shown that alveolar epithelial cells can also produce CXCL2 in response to pathogens (49). Additionally, we focused on neutrophil recruitment mediated by CXCL2 as it is the earliest event in the development of PGD. However, our current and previously published data suggest that the development of PGD involves several cell populations including non-classical monocytes, neutrophils, alveolar macrophages and classical monocytes. The complex signaling pathways leading to their orchestrated sequential recruitment and activation are incompletely understood. While we show a clear role for retained endotoxin from different bacterial pathogens in neutrophil recruitment after transplant, our findings do not exclude the possibility that damage-associated molecular patterns (DAMPs), such as HMGB1, might be released during the ischemia-reperfusion phase and also trigger TLR activation

(50, 51). Finally, the lung microbiome did not reveal significant differences between the pathogenic and non-pathogenic bacteria making it less likely to account for PGD outcomes. Furthermore, these organisms would likely be cleared by the broad-spectrum antibiotics that are administered routinely to the donor prior to transplant and the recipient after transplant.

In conclusion, we show that contamination of donor lungs with levels of LPS insufficient to induce detectable injury prior to transplantation induces TLR4/MyD88 signaling in ischemia-reperfusion primed TRAM to release CXCL2 leading to neutrophil recruitment. This priming of donor TRAM is independent of the requirement for NCM to recruit neutrophils to lung allografts from naïve donors after lung transplantation. Our results highlight the potential utility of strategies targeting CXCL2, scavenging ROS, or blocking TLR4 or co-receptor CD14 on donor TRAM and NCM to reduce neutrophil recruitment and PGD in endotoxin containing donor lungs.

Methods

Human samples

Transplant patients. Bronchoscopic bronchoalveolar lavage and lung biopsies were used to collect donor TRAM at the different time points outlined in the experiments.

Pseudomonas aeruginosa infected patients. Small aliquot (1-4 mLs) of non-bronchoscopic bronchoalveolar lavage (NBBAL) fluid were collected from patients with suspected infection (16).

Bronchoalveolar lavage fluid (BALF) processing. Fluid was filtered through a 40-µ nylon cell strainer and following staining, cells were sorted at the Northwestern University Robert H. Lurie Comprehensive Cancer Center Flow Cytometry Core facility using FACSARIA III, BD. Tissue-resident TRAM were identified using sequential gating as singlets/$CD45^{+}$/live/$CD15^{-}$ /$CD206^{++}$/$CD169^{+}$/HLA-DR^{+}/high $autofluorescence^{+}$ as previously described (16).

Mice and procedures

Wild type C57BL/6J (B6), B6.FVB-Tg(ITGAMDTR/EGFP)- 34Lan/J (CD11b-DTR) and *Rag*$^{-/-}$ *IL2g*$^{-/-}$ mice with transgenes for human *GM-CSF* and *IL-3* (MSTRG mice) (16), *Cxcr2*$^{-/-}$ *and Nr4a1*$^{-/-}$ mice were obtained from Jackson Laboratory. *Tlr4*$^{-/-}$ and *Cd11c*^{Cre}*Myd88*$^{\Delta}$ mice in B6 background were a gift from Prof. Harris Perlman (Department of Medicine, Northwestern University, Chicago) and *B6 lysozyme M (LysM)–GFP* mice were originally obtained from Prof. Klaus Ley (La Jolla Institute for Immunology, California). All mice were maintained in a specific pathogen-free facility at the Center for Comparative Medicine at Northwestern University and used for the described experiments at the age of 9-14 weeks and between 24-28 g of body weight.

LPS induced lung injury: LPS from *Escherichia coli* (serotype O111:B4; Sigma-Aldrich), *Pseudomonas aeruginosa 10* (serotype 10.22; Sigma-Aldrich) and *Klebsiella pneumoniae* (source strain ATCC 15380; Sigma-Aldrich) were used at 2 µg/g B.W. (body weight) or 0.5 µg/g

B.W. (*E. coli*) and 0.2 µg/g B.W. *P. aeruginosa* and *K. pneumoniae* diluted in 50 µl of PBS and instilled intratracheally. MISTRG mice reconstitution and mouse pneumonia model were previously described (16).

Broncho alveolar lavage fluid (BALF) was obtained by instilling lung airways 5 times with 0.5 ml PBS. BALF was centrifuged, and the supernatant was used for chemokine and cytokine determination as below described.

Purified Anti-CXCL2 (Clone # 40605; R&D Systems) or rat IgG2B isotype control (R&D Systems), TAK-242, TLR4 antagonist (AbMole), IAXO-101, CD14/TLR4 antagonist (Innaxon), N-acetyl-cysteine (NAC) (Millipore-Sigma), Mito-Tempo (MT) (Sigma-Aldrich) and dimethyl malonate (DM) (Sigma-Aldrich) were commercially acquired. Anti-CXCL2 antibodies or isotype control (200 ug/ms, i.v), TAK-242 (1 ug/g of BW, i.v) and IAXO-101 (3 ug/g of BW, IT) were administrated 30 min prior to IT-LPS to the donors (52, 53). For ROS scavenger experiments, donor mice were treated with the first dose of the NAC (100 mg/kg of BW, i.v), MT (5 mg/kg/ms, i.p) or DM (10 mg/kg of BW, i.v) 1 h prior to transplant; then, recipient mice received same doses of ROS scavenger 5 min prior to reperfusion 1 h (NAC) or 2 h (TM and DM) after reperfusion.

Mouse lung transplant with and without LPS. Orthotopic murine left lung transplantation was performed as previously described (13). Briefly, donor mouse was anesthetized with a mixture of xylazine (10 mg/ kg) and ketamine (100 mg/kg). Donor lungs were flushed through the pulmonary artery with 3 ml of saline solution and the heart-lung block was excised and kept in cooled (4ºC) preservative solution. The bronchus, pulmonary vein, and artery were dissected and prepared for anastomosis. A customized cuff made of a Teflon intravenous catheter was applied to the vascular structures and fixated with a 10-0 nylon ligature. After placement of a microvessel clip on the bronchus to avoid airway infiltration with preservative solution, the graft was stored at 4ºC for a period of 90-120 minutes of cold ischemic time prior to implantation. The recipient mouse

received subcutaneous buprenorphine (0.1 mg/kg) 30 min prior to the thoracic surgical incision and every 6 h as needed after the transplant procedure. The recipient mouse was intubated and a left-sided thoracotomy was performed within the third intercostal space. The recipient's native lung was gently clamped and pulled out of the thoracic cavity. The space between the artery, the vein and the bronchus was dissected separately. The artery and vein were temporarily occluded using 8-0 nylon ligatures. The anastomoses were completed by fixating each cuff with 10-0 nylon ligatures. The 8-0 ligatures were released (first vein, then artery) and the lung inflated. The chest incision was closed and recipients separated from the ventilator when spontaneous respiration resumed. No antibiotics or immunosuppressive agents were used postoperatively in any groups. For LPS-treated donors with or without TLR4 or CD14 antagonist, we treated donor mice 30 minutes prior to procurement with 0.5 µg/g/BW IT-LPS with or without 100 µg/ms/i.v, respectively.

Adoptive transfer of TRAM. A tracheostomy was performed in the donor mice to harvest TRAM from BALF. Briefly, BALF was obtained with 2mM EDTA solution in PBS lavage following by centrifugation and red blood cell (RBC) lysis. TRAM obtained from BAL was resuspended in the final volume for adoptive transfer to the recipient mice $5x10^5$ per recipient.

TRAM and monocytes depletion. Clodronate-loaded liposomes and control phosphate-buffered saline liposomes were purchased from Clodronateliposomes.com. At specific time points, mice were injected IT (50 µl) or IV (200 µl) with clodronate-loaded liposomes or control PBS-loaded liposomes to deplete macrophages or $Ly6C^{hi}$ monocytes, respectively (54). Cytotoxic anti-CCR2 antibodies were a kind gift of Steffen Jung and used for selective depletion of CCR2+ classical monocytes as previously described. Diphtheria toxin (List Biologic Laboratories, Inc.) was dissolved in 100 µL of PBS and administered intraperitoneally to CD11b-DTR mice 24 hours prior to LPS administration to systematically deplete CD11b-expressing cells.

Compartmental Lung Intravenous Staining for Neutrophils Extravasation

Intravenous and intratracheal procedure was performed utilizing an adaptation of previously described methods (34). Briefly, 6μg of APC-conjugated anti-CD45 in 100ul of sterile PBS was injected IV and allowed to circulate for 3 minutes prior to euthanasia with an overdose of Euthasol. Tracheostomy was performed. The vena cava was transected and the right ventricle flushed with 10mL of HBSS to wash unbound IV antibody.

Multicolor flow cytometry

Single cell suspensions from the whole lung of the mouse were obtained and murine lung cell staining performed as previously described (32, 55). Fixed samples were run on a custom LSRFortessa Cell Analyzer (BD) or BD FACS Symphony A5-Laser Analyzer for flow cytometry analysis at the Northwestern University Robert H. Lurie Comprehensive Cancer Center Flow Cytometry Core facility. Acquired data was analyzed with FlowJo v10.6 (FlowJo). For TRAM sorting, lung airways were lavaged 5 times with 0.5 ml PBS. BALF was centrifuged, and the cell pellet was processed and prepared for flow sorting using a FACSARIA 4-Laser Sorter at the Northwestern University Robert H. Lurie Comprehensive Cancer Center Flow Cytometry Core facility.

Wet/dry ratio

Weight Ratio for Pulmonary Edema was measured by harvesting lungs after reperfusion at defined experiments, weighed, and then placed at 54°C until a stable dry weight was achieved. The ratio of wet weight to dry weight was calculated as an indicator of pulmonary edema.

Histology and H&E staining

For histological analyses, the whole lung was harvested and gently flushed through the pulmonary artery with 3ml saline. 4% paraformaldehyde was instilled into the trachea with a pressure of 10 cmH_2O then fixed for 48-72 hours prior to being embedded in paraffin. The whole lung was serially sectioned and stained with hematoxylin and eosin (H&E). Pictures were acquired using a Nikon TE-2000-U microscope.

ELISA

Endotoxin (Thermo Fisher), CXCL1, CXCL2, CXCL10 and TNFα ELISA was performed using a commercially available kit accordingly to manufacturer's instructions (R&D Systems).

Secondary transcriptomic analysis

*RNA-sequencing***:** RNA isolation and sequencing procedures are detailed in our manuscript (34). For all analyses, normalized tables of counts were generated from raw counts using the EdgR package (version 3.18.1). Filtering for low counts was performed by excluding genes which have the expression from more than half of all the samples. Functional enrichment analysis with GO biological processes was performed with GOrilla with the top 1000 genes upregulated in *P. aeruginosa* positive samples for all clusters. Significantly upregulated genes were used to identify the top biological processes (-log 10 (p-value)). Heatmap of pathway genes based on the top GO processes identified and hierarchical clustering generated to show the expression of these genes in naïve, low and high virulence samples for MISTRG mice (16).

Re-analysis of single cell RNA-seq datasets. To assess expression pattern of *TRL4* in human lung we queried three recently published single cell RNA-seq datasets (29,30,31). Data and author's annotations were accessed from GSE122960 (29), tissuestabilitycellatlas.org (30) and GSE135893 (31). Only non-diseased lungs (indicated as "Donor" or "Control") were used for

analysis. Precomputed R objects were loaded into Seurat 3.1.4 and expression of *TLR4* was visualized using FeaturePlot command.

Two-Photon Microscopy

A custom built 2P microscope running ImageWarp acquisition software (A&B Software) was used for time-lapse imaging. Mice were anesthetized with an intraperiteonal injection of ketamine (50 mg/kg) and xylazine (10 mg/kg) and maintained with administration of half doses every hour through the imaging process. Mice were intubated orotracheally and ventilated with room air at a rate of 120 breaths/min and with a tidal volume of 0.5 mL. Left thoracotomy was performed to expose the left lung, and the lung was imaged using a custom-built chamber maintained at 37 °C. VetBond ring was used to attach the lung tissue to the bottom of the cover glass without direct pressure on the exposed lung. For time-lapse imaging of leukocyte migration in the tissue parenchyma, we averaged 15 video-rate frames (0.5 s per slice) during the acquisition to match the ventilator rate and minimize movement artifacts. Each plane represents an image of 220 × 240 μm in the x and y dimensions. To visualize blood vessels, 20 μL of 655-nm nontargeted Q-dots in 100 μL of PBS were injected i.v prior to imaging. Two-photon excitation produces a second harmonic signal from collagen (56) around alveoli, thus providing a useful landmark for the air spaces. Explanted tissue was examined as described (56-58).

mRNA isolation and qPCR.

Total RNA was extracted using miRNeasy Mini kit (Qiagen). cDNA was synthesized from 1μg of total RNA by using a qScript™ cDNA Synthesis kit (Quanta Biosciences) and mRNA expression was determined by qPCR using iTaq Universal Probes Supermix (BioRad). Relative expression of the transcripts was determined according to the ΔΔCt method using actin or RPL19 as reference for normalization. Primers used*: cxcl2*-F: CCCAGACAGAAGTCATAGCCAC; *cxcl2*-R: GCCTTGCCTTTGTTCAGTATC); *tlr4*-F: TGGCTGGTTTACACATCCATCGGT; *tlr4*-R:

TGGCACCATTGAAGCTGAGGTCTA; *B-actin*-F: CACCACACCTTCTACAATGA; *B-actin*-R: GTCTCAAACATGATCTGGGT.

Reactive Oxygen Species measurement

The ROS levels were examined in lung samples using a commercially available assay (In vitro OxiSelect Assay Kit, Cell Biolabs, San Diego, CA). Briefly, we homogenized the lung tissue obtained at the different time points during the lung transplantation (native donor lung pre-perfusion, cold-ischemia, warm-ischemia, post-reperfusion 30 minutes) according to the manufacturer's recommendation and resuspended it in the assay buffer. The cell permeable fluorogenic probe was then used to assess the ROS levels. Fluorescence was read on a Spectramax plate reader.

Immunocytochemistry and Fluorescent microscopy

10,000-50,000 TRAM were cytospined into slides, fixed with 4% formaldehyde, permeabilized with 0.5% Triton X-100 and immunostained with anti-PE-TLR4 antibody (BioLegend, clone HTA125). Nuclei were stained with Hoechst 33342 (Sigma). For immunocytochemistry, cells were imaged using a Zeiss Axioplan 2 fluorescence microscope. Confocal images were acquired using a Zeiss Axio Imager Z2 with ApoTome.2 microscope equipped with Axiocam 503 Mono, X-Cite 120 LED Boost System, and Zen 2.3 software (Carl Zeiss, Oberkochen, Germany).

Microbiome analysis

Ten bronchoalveolar lavage (BAL) washings of donor lungs were obtained in the operating room at the time of organ implantation. Rectal swabs were obtained for five of these patients at the same time. Samples were immediately centrifuged to collect cellular DNA and stored at -80° C. Samples then underwent batched genomic DNA extraction, PCR-amplification targeting the 16S ribosomal RNA gene, pooling, and high-throughput sequencing with paired-end, 300 base reads on the Illumina MiSeq platform to obtain overall taxonomic compositions of the microbial communities. A sterile swab obtained just prior to DNA extraction was used for the negative

control. Distances for each sample's overall microbial profile were generated via square root transformation of the relative abundances of each taxon. A non-metric multidimensional scaling plot was created by using Bray-Curtis dissimilarity through PRIMER version 7 as shown in Supplemental Figure 2. 2D stress was 0.14. An analysis of similarity (ANOSIM) was used to determine statistical similarities between groups.

TRAM viability in vitro

TRAM viability were measured with Acridine Orange/Propidium Iodide (AO/PI) nucleic acid binding dyes method using Nexcelom cellometer. AO is cell permeable, all stained nucleated cells generate a green fluorescence and PI only enters cells with compromised membranes and therefore dying, dead and necrotic nucleated cells stained with PI generate a red fluorescence. Cell viability is calculated by examining the ratio of the number of live to the number of dead fluorescing cells (Nexcelom).

Statistics.

Data analysis was performed using Prism 8 (GraphPad Software). Results are expressed as mean ± SD and the n values for each data set are provided in the figure legends. Statistical significance was assessed by 2-tailed Student's t test, or one-way ANOVA followed by Tukey's post-hoc test. A P value less than 0.05 was considered significant.

Study approval.

All procedures were approved by The Institutional Animal Care and Use (IS00002248) at Northwestern University. Animals received humane care in compliance with the NIH Guide for the Care and Use of Laboratory Animals and the Principles of Laboratory Animal Care formulated by the National Society for Medical Research. Human protocol was part of the Northwestern University Institutional Review Board (STU00106589 and STU00201397). All study subjects provided informed consent.

Author contributions

M.A and E.L. contributed to conceptualization, study design and methodology, data collection and formal analysis and manuscript writing. S.F.C., R.F, S.M., T.M., and J.W. contributed to formal analysis, methodology and drafting the manuscript. Q.W. H.S., S.R., W.L, A.H. conducted experiments. N. J. and Z.R., contributed to formal analysis and methodology. D.K., M.Q, A.V.M., F.L.N.S., S.Ro. and C.K. contributed to methodology, validation, formal analysis, and visualization. G.R.S.B. and A.B., contributed to conceptualization, methodology, validation, formal analysis, investigation, resources, data curation, writing, visualization, supervision, project administration, and funding acquisition.

Acknowledgements

This work was supported by NIH HL145478, HL147290, HL147575 (to AB), NIH P01 AG049665, NIH P01 HL071643, Department of the Army W81XWH-15-1-0215 (to GRSB, and AVM), and 5P01AG049665, 5P01HL071643 to N.S.C. The Northwestern University Flow Cytometry Core Facility is supported by Cancer Center Support Grant (NCI CA060553). We thank Suchitra Swaminathan, director of the Flowcytometry core facility, for providing professional technical assistance and Ms. Elena Susan for administrative assistance and submission of the manuscript.

References

1. Charlson ES, Bittinger K, Haas AR, Fitzgerald AS, Frank I, Yadav A, et al. Topographical continuity of bacterial populations in the healthy human respiratory tract. *Am J Respir Crit Care Med.* 2011;184(8):957-63.
2. Huang YJ, Charlson ES, Collman RG, Colombini-Hatch S, Martinez FD, and Senior RM. The role of the lung microbiome in health and disease. A National Heart, Lung, and Blood Institute workshop report. *Am J Respir Crit Care Med.* 2013;187(12):1382-7.
3. Ruiz I, Gavalda J, Monforte V, Len O, Roman A, Bravo C, et al. Donor-to-host transmission of bacterial and fungal infections in lung transplantation. *Am J Transplant.* 2006;6(1):178-82.
4. Abraham E. Neutrophils and acute lung injury. *Crit Care Med.* 2003;31(4 Suppl):S195-9.
5. Puljic R, Benediktus E, Plater-Zyberk C, Baeuerle PA, Szelenyi S, Brune K, et al. Lipopolysaccharide-induced lung inflammation is inhibited by neutralization of GM-CSF. *Eur J Pharmacol.* 2007;557(2-3):230-5.
6. Chabot F, Mitchell JA, Gutteridge JM, and Evans TW. Reactive oxygen species in acute lung injury. *Eur Respir J.* 1998;11(3):745-57.
7. Saffarzadeh M, Juenemann C, Queisser MA, Lochnit G, Barreto G, Galuska SP, et al. Neutrophil extracellular traps directly induce epithelial and endothelial cell death: a predominant role of histones. *PLoS One.* 2012;7(2):e32366.
8. Narasaraju T, Yang E, Samy RP, Ng HH, Poh WP, Liew AA, et al. Excessive neutrophils and neutrophil extracellular traps contribute to acute lung injury of influenza pneumonitis. *Am J Pathol.* 2011;179(1):199-210.
9. Williams AE, and Chambers RC. The mercurial nature of neutrophils: still an enigma in ARDS? *Am J Physiol Lung Cell Mol Physiol.* 2014;306(3):L217-30.

10. Kreisel D, Sugimoto S, Tietjens J, Zhu J, Yamamoto S, Krupnick AS, et al. Bcl3 prevents acute inflammatory lung injury in mice by restraining emergency granulopoiesis. *J Clin Invest.* 2011;121(1):265-76.

11. Bharat A, and Kreisel D. Immunopathogenesis of Primary Graft Dysfunction After Lung Transplantation. *Ann Thorac Surg.* 2018;105(3):671-4.

12. Hsiao HM, Fernandez R, Tanaka S, Li W, Spahn JH, Chiu S, et al. Spleen-derived classical monocytes mediate lung ischemia-reperfusion injury through IL-1beta. *J Clin Invest.* 2018;128(7):2833-47.

13. Zheng Z, Chiu S, Akbarpour M, Sun H, Reyfman PA, Anekalla KR, et al. Donor pulmonary intravascular nonclassical monocytes recruit recipient neutrophils and mediate primary lung allograft dysfunction. *Sci Transl Med.* 2017;9(394).

14. Chignard M, and Balloy V. Neutrophil recruitment and increased permeability during acute lung injury induced by lipopolysaccharide. *Am J Physiol Lung Cell Mol Physiol.* 2000;279(6):L1083-90.

15. Bharat A, McQuattie-Pimentel AC, and Budinger GRS. Non-classical monocytes in tissue injury and cancer. *Oncotarget.* 2017;8(63):106171-2.

16. Walter JM, Ren Z, Yacoub T, Reyfman PA, Shah RD, Abdala-Valencia H, et al. Multidimensional Assessment of the Host Response in Mechanically Ventilated Patients with Suspected Pneumonia. *Am J Respir Crit Care Med.* 2019;199(10):1225-37.

17. Maus UA, Waelsch K, Kuziel WA, Delbeck T, Mack M, Blackwell TS, et al. Monocytes are potent facilitators of alveolar neutrophil emigration during lung inflammation: role of the CCL2-CCR2 axis. *J Immunol.* 2003;170(6):3273-8.

18. Dhaliwal K, Scholefield E, Ferenbach D, Gibbons M, Duffin R, Dorward DA, et al. Monocytes control second-phase neutrophil emigration in established lipopolysaccharide-induced murine lung injury. *Am J Respir Crit Care Med.* 2012;186(6):514-24.

19. Beck-Schimmer B, Schwendener R, Pasch T, Reyes L, Booy C, and Schimmer RC. Alveolar macrophages regulate neutrophil recruitment in endotoxin-induced lung injury. *Respir Res.* 2005;6:61.

20. Bhatia M, Zemans RL, and Jeyaseelan S. Role of chemokines in the pathogenesis of acute lung injury. *Am J Respir Cell Mol Biol.* 2012;46(5):566-72.

21. Becker J, Poroyko V, and Bhorade S. The lung microbiome after lung transplantation. *Expert Rev Respir Med.* 2014;8(2):221-31.

22. Mitchell AB, and Glanville AR. The Human Respiratory Microbiome: Implications and Impact. *Semin Respir Crit Care Med.* 2018;39(2):199-212.

23. Wu Q, Turturice B, Wagner S, Huang Y, Gupta PK, Schott C, et al. Gut Microbiota Can Impact Chronic Murine Lung Allograft Rejection. *Am J Respir Cell Mol Biol.* 2019;60(1):131-4.

24. Guo Y, Wang Q, Li D, Onyema OO, Mei Z, Manafi A, et al. Vendor-specific microbiome controls both acute and chronic murine lung allograft rejection by altering CD4(+) Foxp3(+) regulatory T cell levels. *Am J Transplant.* 2019;19(10):2705-18.

25. Moffatt MF, and Cookson WO. The lung microbiome in health and disease. *Clin Med (Lond).* 2017;17(6):525-9.

26. Tsai MH, Liu YY, and Chen CC. OutbreakFinder: a visualization tool for rapid detection of bacterial strain clusters based on optimized multidimensional scaling. *PeerJ.* 2019;7:e7600.

27. Grommes J, and Soehnlein O. Contribution of neutrophils to acute lung injury. *Mol Med.* 2011;17(3-4):293-307.

28. Faller S, Hausler F, Goeft A, von Itter MA, Gyllenram V, Hoetzel A, et al. Hydrogen sulfide limits neutrophil transmigration, inflammation, and oxidative burst in lipopolysaccharide-induced acute lung injury. *Sci Rep.* 2018;8(1):14676.

29. Reyfman PA, Walter JM, Joshi N, Anekalla KR, McQuattie-Pimentel AC, Chiu S, et al. Single-Cell Transcriptomic Analysis of Human Lung Provides Insights into the Pathobiology of Pulmonary Fibrosis. *Am J Respir Crit Care Med.* 2019;199(12):1517-36.

30. Madissoon E, Wilbrey-Clark A, Miragaia RJ, Saeb-Parsy K, Mahbubani KT, Georgakopoulos N, et al. scRNA-seq assessment of the human lung, spleen, and esophagus tissue stability after cold preservation. *Genome Biology.* 2019;21(1):1.

31. Habermann AC, Gutierrez AJ, Bui LT, Yahn SL, Winters NI, Calvi CL, et al. Single-cell RNA-sequencing reveals profibrotic roles of distinct epithelial and mesenchymal lineages in pulmonary fibrosis. *bioRxiv.* 2019:753806.

32. Bharat A, Bhorade SM, Morales-Nebreda L, McQuattie-Pimentel AC, Soberanes S, Ridge K, et al. Flow Cytometry Reveals Similarities Between Lung Macrophages in Humans and Mice. *Am J Respir Cell Mol Biol.* 2016;54(1):147-9.

33. Miller SI, Ernst RK, and Bader MW. LPS, TLR4 and infectious disease diversity. *Nat Rev Microbiol.* 2005;3(1):36-46.

34. Koch CM, Chiu SF, Akbarpour M, Bharat A, Ridge KM, Bartom ET, et al. A Beginner's Guide to Analysis of RNA-seq Data. *Am J Respir Cell Mol Biol.* 2018.

35. Powers KA, Szaszi K, Khadaroo RG, Tawadros PS, Marshall JC, Kapus A, et al. Oxidative stress generated by hemorrhagic shock recruits Toll-like receptor 4 to the plasma membrane in macrophages. *J Exp Med.* 2006;203(8):1951-61.

36. Prag HA, Kula-Alwar D, Beach TE, Gruszczyk AV, Burger N, and Murphy MP. In: Sies H ed. *Oxidative Stress*. Academic Press; 2020:513-38.

37. Wu MY, Yiang GT, Liao WT, Tsai AP, Cheng YL, Cheng PW, et al. Current Mechanistic Concepts in Ischemia and Reperfusion Injury. *Cell Physiol Biochem.* 2018;46(4):1650-67.

38. Inci I, Erne B, Arni S, Jungraithmayr W, Inci D, Hillinger S, et al. Prevention of primary graft dysfunction in lung transplantation by N-acetylcysteine after prolonged cold ischemia. *J Heart Lung Transplant.* 2010;29(11):1293-301.

39. Trnka J, Blaikie FH, Smith RA, and Murphy MP. A mitochondria-targeted nitroxide is reduced to its hydroxylamine by ubiquinol in mitochondria. *Free Radic Biol Med.* 2008;44(7):1406-19.

40. Chouchani ET, Pell VR, Gaude E, Aksentijevic D, Sundier SY, Robb EL, et al. Ischaemic accumulation of succinate controls reperfusion injury through mitochondrial ROS. *Nature.* 2014;515(7527):431-5.

41. Young KA, and Dilling DF. The Future of Lung Transplantation. *Chest.* 2019;155(3):465-73.

42. Somers J, Ruttens D, Verleden SE, Cox B, Stanzi A, Vandermeulen E, et al. A decade of extended-criteria lung donors in a single center: was it justified? *Transpl Int.* 2015;28(2):170-9.

43. Courtwright A, and Cantu E. Evaluation and Management of the Potential Lung Donor. *Clin Chest Med.* 2017;38(4):751-9.

44. Mojtabaee M, Shahryari S, and Sadegh Beigee F. Reasons for Donor Lungs Unsuitability After Radiographic Selection. *Exp Clin Transplant.* 2019;17(Suppl 1):120-2.

45. Van Raemdonck DE, Jannis NC, De Leyn PR, Flameng WJ, and Lerut TE. Warm ischemic tolerance in collapsed pulmonary grafts is limited to 1 hour. *Ann Surg.* 1998;228(6):788-96.

46. Geudens N, Van De Wauwer C, Neyrinck AP, Timmermans L, Vanhooren HM, Vanaudenaerde BM, et al. N-acetyl cysteine pre-treatment attenuates inflammatory changes in the warm ischemic murine lung. *J Heart Lung Transplant.* 2007;26(12):1326-32.

47. Tawadros PS, Powers KA, Ailenberg M, Birch SE, Marshall JC, Szaszi K, et al. Oxidative Stress Increases Surface Toll-Like Receptor 4 Expression in Murine Macrophages Via Ceramide Generation. *Shock.* 2015;44(2):157-65.

48. Frevert CW, Huang S, Danaee H, Paulauskis JD, and Kobzik L. Functional characterization of the rat chemokine KC and its importance in neutrophil recruitment in a rat model of pulmonary inflammation. *J Immunol.* 1995;154(1):335-44.

49. Bello-Irizarry SN, Wang J, Olsen K, Gigliotti F, and Wright TW. The alveolar epithelial cell chemokine response to pneumocystis requires adaptor molecule MyD88 and interleukin-1 receptor but not toll-like receptor 2 or 4. *Infect Immun.* 2012;80(11):3912-20.

50. Sharma AK, LaPar DJ, Stone ML, Zhao Y, Kron IL, and Laubach VE. Receptor for advanced glycation end products (RAGE) on iNKT cells mediates lung ischemia-reperfusion injury. *Am J Transplant.* 2013;13(9):2255-67.

51. Paudel YN, Angelopoulou E, Piperi C, Balasubramaniam V, Othman I, and Shaikh MF. Enlightening the role of high mobility group box 1 (HMGB1) in inflammation: Updates on receptor signalling. *Eur J Pharmacol.* 2019;858:172487.

52. Sha T, Sunamoto M, Kitazaki T, Sato J, Ii M, and Iizawa Y. Therapeutic effects of TAK-242, a novel selective Toll-like receptor 4 signal transduction inhibitor, in mouse endotoxin shock model. *Eur J Pharmacol.* 2007;571(2-3):231-9.

53. Haziak K, Herman AP, Wojtulewicz K, Pawlina B, Paczesna K, Bochenek J, et al. Effect of CD14/TLR4 antagonist on GnRH/LH secretion in ewe during central inflammation induced by intracerebroventricular administration of LPS. *J Anim Sci Biotechnol.* 2018;9:52.

54. Van Rooijen N, and Sanders A. Liposome mediated depletion of macrophages: mechanism of action, preparation of liposomes and applications. *J Immunol Methods.* 1994;174(1-2):83-93.

55. Misharin AV, Morales-Nebreda L, Reyfman PA, Cuda CM, Walter JM, McQuattie-Pimentel AC, et al. Monocyte-derived alveolar macrophages drive lung fibrosis and persist in the lung over the life span. *J Exp Med.* 2017;214(8):2387-404.

56. Gelman AE, Li W, Richardson SB, Zinselmeyer BH, Lai J, Okazaki M, et al. Cutting edge: Acute lung allograft rejection is independent of secondary lymphoid organs. *J Immunol.* 2009;182(7):3969-73.

57. Halle S, Dujardin HC, Bakocevic N, Fleige H, Danzer H, Willenzon S, et al. Induced bronchus-associated lymphoid tissue serves as a general priming site for T cells and is maintained by dendritic cells. *J Exp Med.* 2009;206(12):2593-601.

58. Kreisel D, Nava RG, Li W, Zinselmeyer BH, Wang B, Lai J, et al. In vivo two-photon imaging reveals monocyte-dependent neutrophil extravasation during pulmonary inflammation. *Proc Natl Acad Sci U S A.* 2010;107(42):18073-8.

Table 1. Antibodies used for flow cytometry and sorting

Antigen	Clone	Fluorchrome	Manufacturer
CD24	M1/69	BUV395/APC	BD Horizon
CD45	30-F11	FITC/APC	BioLegend
CD11b	M1/70	FITC/APCCy7	BD Horizon/BioLegend
I-A/I-E	M5/114.15.2	FITC/PercpCy5.5	BioLegend
Ly6C	HK 1.4	eFluor450	eBioscience
Ly6G	1A8	AlexaFluor 700	BioLegend
NK1.1	PK136	AlexaFluor 700	BD
CD64	X54-5/7.1	PE	BioLegend
SiglecF	E50-2440	PECF594	BD
CD11c	HL3	PECy7	BD
TLR4	MT5510	PECy7	BioLegend

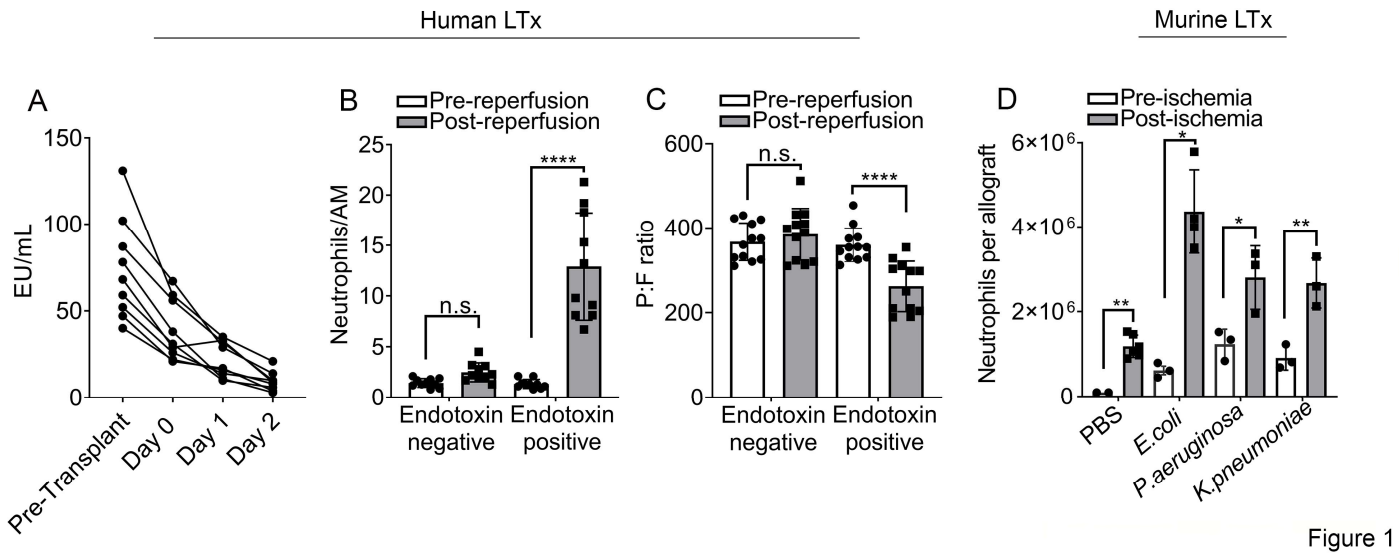
Human LTx
Murine LTx
A
EU/mL
150
100
50
0
Pre-Transplant
Day 0
Day 1
Day 2
B
Pre-reperfusion
Post-reperfusion
Neutrophils/AM
25
20
15
10
5
0
n.s.
****
Endotoxin negative
Endotoxin positive
C
Pre-reperfusion
Post-reperfusion
P:F ratio
600
400
200
0
n.s.
****
Endotoxin negative
Endotoxin positive
D
Pre-ischemia
Post-ischemia
Neutrophils per allograft
6×10^6
4×10^6
2×10^6
0
**
*
*
**
PBS
E.coli
P.aeruginosa
K.pneumoniae

Figure 1

Figure 1. Persistence of endotoxin in human and murine donor lungs is associated with neutrophil influx and PGD following transplantation. (A) Human donor lungs with microbial cultures positive for gram-negative bacteria were treated with antimicrobials resulting in clearance of the pathogen at the time of transplantation. To test for persistence of endotoxin, bronchoalveolar lavage fluid serially obtained from the same patient was analyzed (n=9). (B) Human donor lungs from endotoxin-negative and endotoxin-positive lungs were analyzed for tissue neutrophil infiltration pre-reperfusion and 30 min following reperfusion using intraoperative lung biopsy of the inferior lingular segment (n=10). (C) To determine the function of the lung allograft, we obtained blood directly from the pulmonary vein confluence immediately proximal to the site of venous anastomosis and analyzed partial pressure of oxygen (PaO_2 mmHg) before and after reperfusion. The PaO_2 to fractional inspired oxygen (FiO_2) ratio (P:F ratio) was then calculated for lungs negative and positive for endotoxin (n=12). (D) Donor mice were administered low dose of lipopolysaccharide intratracheally (*E.coli* (0.5 µg/g BW), *P.aeruginosa* (0.2 µg/g BW) and *K. pneumoniae* (0.2 µg/g BW)), insufficient to cause injury in native lung, and then transplanted into allogeneic recipients. The neutrophil infiltration was then analyzed following transplant (n=3-6). Graphs show means ± SD. Graphs were analyzed by unpaired t-test. n.s. not significant; *p<0.05; **p<0.01; ****p<0.0001.

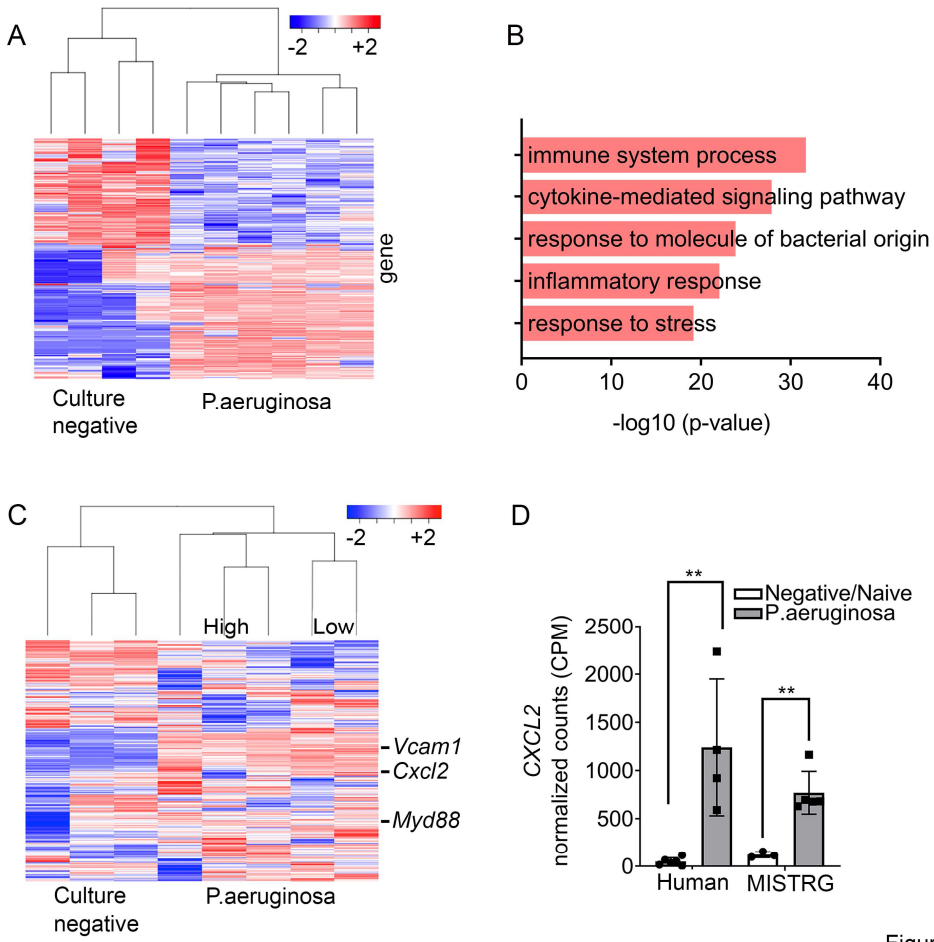
A
-2
+2
gene
Culture negative
P.aeruginosa
B
immune system process
cytokine-mediated signaling pathway
response to molecule of bacterial origin
inflammatory response
response to stress
0
10
20
30
40
-log10 (p-value)
C
-2
+2
High
Low
Vcam1
Cxcl2
Myd88
Culture negative
P.aeruginosa
D
**
**
Negative/Naive
P.aeruginosa
CXCL2 normalized counts (CPM)
2500
2000
1500
1000
500
0
Human
MISTRG

Figure 2

Figure 2. Tissue resident alveolar macrophages upregulate CXCL2 in response to endotoxin and pseudomonas. Transcriptomic profiling of human tissue resident alveolar macrophage (TRAM) during gram-negative bacterial pneumonia revealed upregulation of CXCL2, a known neutrophil chemoattractant. TRAM were identified as $CD15^{-}HLA^{-}DR^{+}CD169^{+}CD206^{++}$, and flow sorted for RNA isolation, library preparation and sequencing (culture negative n=4 and *P.aeruginosa* positive n=6). (A) Heatmap of top 1000 most significantly differentially expressed genes ranked by FDR q-value. Both samples and genes are grouped by hierarchical clustering. (B) Functional enrichment analysis with GO biological processes was performed with GOrilla with the top 1000 genes upregulated in *P.aeruginosa* positive samples for all clusters. In total, 443 significantly upregulated genes were used to identify the top 5 biological processes (-log 10 (p-value)). (C) Heatmap of pathway genes (750 genes) based on the top GO processes identified in (B) (GO:0002376,GO:0019221, GO:0002237,GO:0006954,GO:0006950). Hierarchical clustering shows the expression of these genes in naïve, low and high virulence samples for MISTRG mice. Selective genes are highlighted (n=3-4). (D) Normalized CPM counts of CXCL2 in both human and MISTRG mouse following infection with *P. aeruginosa* (n=3-6). Graph show means ± SD and was analyzed by unpaired t-test.**p<0.01.

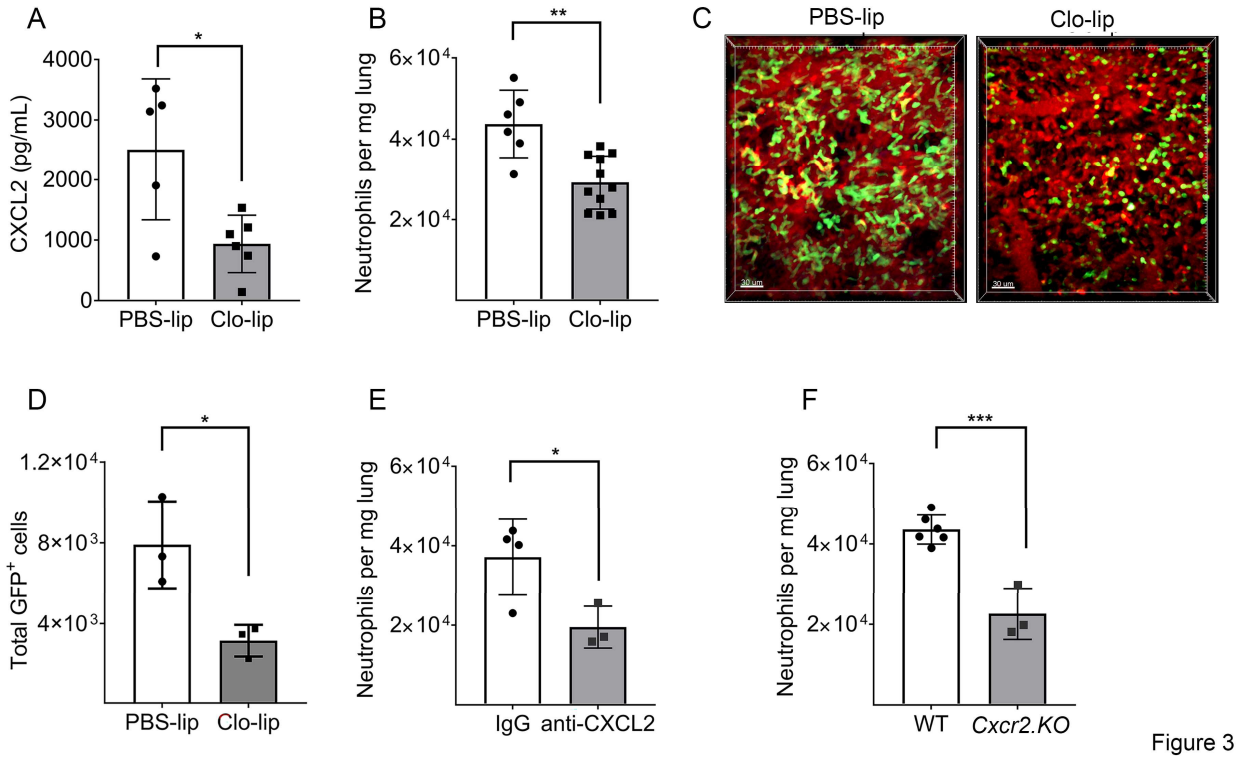
A
CXCL2 (pg/mL)
4000
3000
2000
1000
0
*
PBS-lip
Clo-lip
B
Neutrophils per mg lung
6×10^4
4×10^4
2×10^4
**
PBS-lip
Clo-lip
C
PBS-lip
Clo-lip
D
Total GFP+ cells
1.2×10^4
8×10^3
4×10^3
*
PBS-lip
Clo-lip
E
Neutrophils per mg lung
6×10^4
4×10^4
2×10^4
*
IgG
anti-CXCL2
F
Neutrophils per mg lung
6×10^4
4×10^4
2×10^4
***
WT
Cxcr2.KO

Figure 3

Figure 3. Influx of neutrophils into LPS-treated lung is abrogated by selective depletion of TRAM. (A) CXCL2 chemokine levels in BALF of LPS-treated mice and injected with PBS-lip or Clo-lip intratracheally (n =5-6). (B) Quantification of neutrophil infiltration into lungs in TRAM-depleted compared to PBS-lip control mice 24 h following LPS administration (n=6-11). Neutrophils were gated on live $CD45^{+}Ly6G^{+}CD11b^{+}CD24^{+}SSC^{hi}$. (C) Representative intravital two-photon microscopy images of control PBS-lip or Clo-lip-treated lungs 4 h after LPS administration in B6 LysM-GFP mice (also refer to videos S1 and S2). Quantum dots 655 were injected 5 min prior to imaging to label the vessels red (n=3). (D) Quantification of total GFP^{+} neutrophils from (C) (n=3). (E) Quantification of neutrophil infiltration into lungs in LPS-treated mice previously injected with IgG or an antibody against CXCL2 (n=3-4). (F) Quantification of neutrophil infiltration into lungs in LPS-treated mice in wild-type (WT) compared to *Cxcr2*$^{-/-}$ (*Cxcr2.KO*) mice (n=3-6). Bar = 30 µm. All graphs show means ± SD. Graphs were analyzed by unpaired t-test. *p<0.05; **p<0.01;***p<0.001.

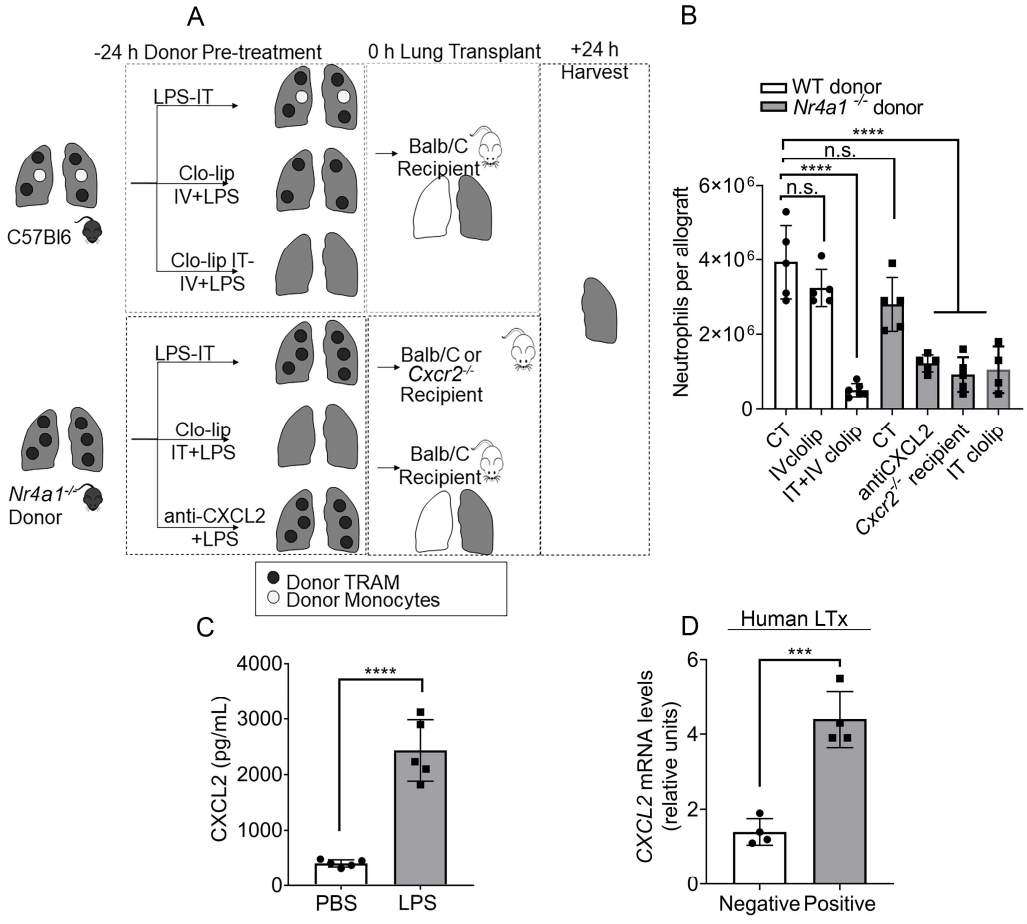
A
-24 h Donor Pre-treatment
0 h Lung Transplant
+24 h Harvest
LPS-IT
Clo-lip IV+LPS
Clo-lip IT-IV+LPS
C57Bl6
Balb/C Recipient
LPS-IT
Clo-lip IT+LPS
anti-CXCL2 +LPS
Nr4a1-/- Donor
Balb/C or Cxcr2-/- Recipient
Balb/C Recipient
Donor TRAM
Donor Monocytes
B
WT donor
Nr4a1 -/- donor
Neutrophils per allograft
6×10^6
4×10^6
2×10^6
0
n.s.
n.s.
****
****
CT
IVclolip
IT+IV clolip
CT
antiCXCL2 Cxcr2-/- recipient
IT clolip
C
CXCL2 (pg/mL)
4000
3000
2000
1000
0
****
PBS
LPS
D
Human LTx
CXCL2 mRNA levels (relative units)
6
4
2
0
***
Negative
Positive

Figure 4

Figure 4. Influx of recipient neutrophils into the allograft containing LPS is abrogated by depletion of donor TRAM and is CXCL2 dependent. (A) Diagram depicting experiment shown in (B). Wild-type C57Bl/6 mice received Balb/c allogeneic donor lungs containing low dose LPS (0.5µg/g BW) injected intratracheally (IT), insufficient to cause native lung injury. To deplete donor non-classical monocytes donors were treated with intravenous (IV) Clolip and then transplanted the LPS containing donor lungs. To deplete both donor monocytes and donor TRAM we treated the donors with IV Clolip and IT Clo-lip, respectively, and then transplanted these donor lungs containing LPS. Next, we used *Nr4a1*$^{-/-}$ donor lungs containing low dose LPS and transplanted them into WT recipients after depletion of TRAM using IT Clo-lip, or PBS-lip as control. Lastly, to determine whether CXCL2 secretion by donor TRAM leads to neutrophil recruitment, we treated recipients of *Nr4a1*$^{-/-}$ donor lungs containing low dose LPS with anti-CXCL2 antibodies at the time of transplantation. Additionally, we transplanted *Nr4a1*$^{-/-}$ donor lungs containing low dose LPS into *Cxcr2*$^{-/-}$ recipients and determined neutrophil infiltration at 24 h.(B) Quantification of neutrophil infiltration into lungs after these treatments was performed using flow-cytometry (n=4-5). (C) CXCL2 chemokine levels in BALF of recipient mice after receiving low dose LPS-treated *Nr4a1*$^{-/-}$ donor lung compared to PBS-treated *Nr4a1*$^{-/-}$ donor lungs (n =5). (D) TRAM were isolated from endotoxin negative and positive human donor lungs at 120 min following reperfusion and analyzed for CXCL2 transcription (n=4). All graphs show means ± SD. Graph on (B) was analyzed by one-way Anova followed by Tukey's post-hoc test. Graphs in (C) and (D) were analyzed by unpaired t-test. n.s. not significant; ***p<0.01; ****p<0.0001. CT= Control.

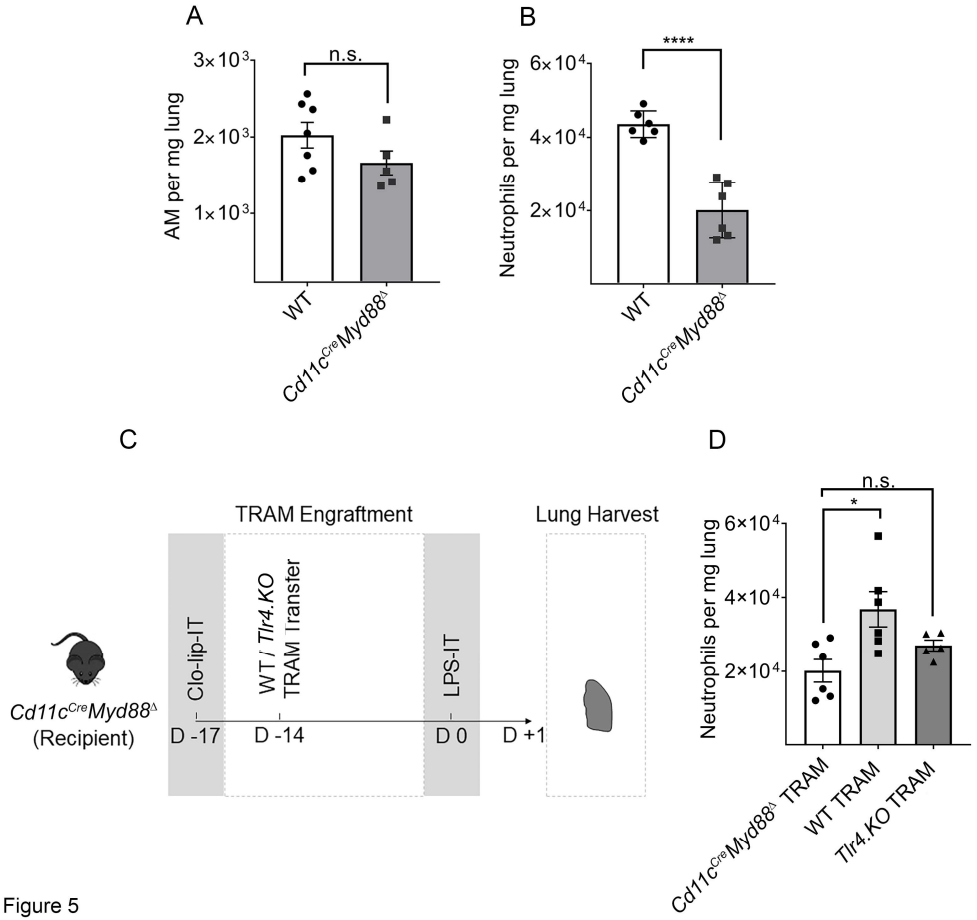
A
n.s.
AM per mg lung
3×10³
2×10³
1×10³
WT
Cd11c^Cre Myd88^Δ
B
****
Neutrophils per mg lung
6×10⁴
4×10⁴
2×10⁴
WT
Cd11c^Cre Myd88^Δ
C
TRAM Engraftment
Lung Harvest
Clo-lip-IT
WT / Tlr4.KO TRAM Transfer
LPS-IT
Cd11c^Cre Myd88^Δ (Recipient)
D -17
D -14
D 0
D +1
D
n.s.
*
Neutrophils per mg lung
6×10⁴
4×10⁴
2×10⁴
Cd11c^Cre Myd88^Δ TRAM
WT TRAM
Tlr4.KO TRAM

Figure 5

Figure 5. TLR4-MyD88 signaling directs TRAM-mediated neutrophil recruitment. (A) Flow cytometry quantification of TRAM in WT and *Cd11c*^{Cre}*Myd88*$^{\Delta}$ mice (n=5-7). TRAM were gated as live CD45^{+}Ly6G^{-}NK1.1^{-}SiglecF^{+}CD64^{+}. (B) Flow cytometry quantification of neutrophil (live CD45^{+}Ly6G^{+}CD11b^{+}CD24^{+}SSC^{hi}) infiltration into lungs after intratracheal (IT) LPS (2µg/g BW) in *Cd11c*^{Cre}*Myd88*$^{\Delta}$ compared to control WT mice (n=6). (C) Diagram depicting TRAM reconstitution experiment shown in (D). (D) Flow cytometry quantification of neutrophil infiltration into lungs determined as in (B) after LPS-IT (2µg/g BW) in *Cd11c*^{Cre}*Myd88*$^{\Delta}$ mice reconstituted with WT (WT TRAM) or *Tlr4*$^{-/-}$ TRAM (*Tlr4.KO* TRAM) compared to *Cd11c*^{Cre}*Myd88*$^{\Delta}$ mice (n=5-6). All graphs show means ± SD. (A) and (B) graphs were analyzed by unpaired t-test. (C) Graph was analyzed by one-way Anova followed by Tukey's post-hoc test. n.s. not significant; *p,0.05; ****p<0.0001.

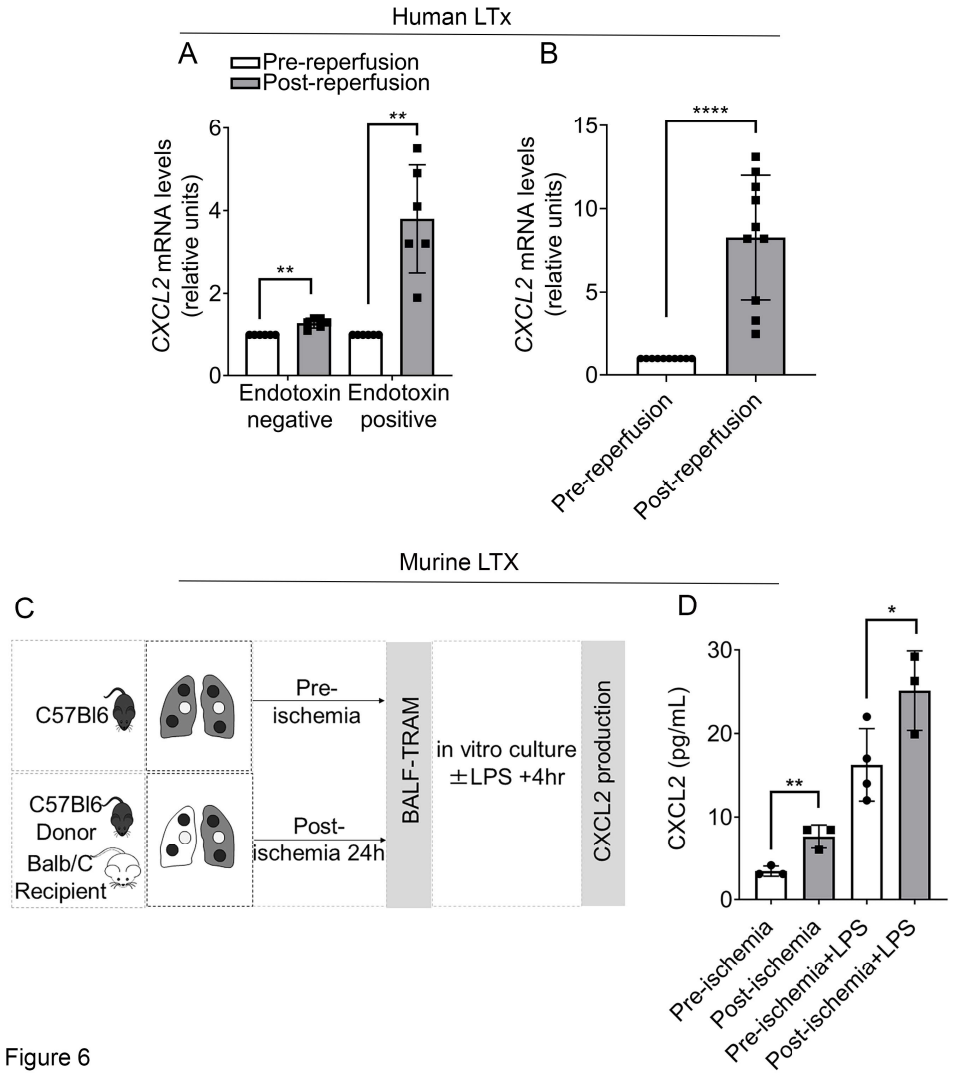
Human LTx
A
Pre-reperfusion
Post-reperfusion
CXCL2 mRNA levels (relative units)
Endotoxin negative
Endotoxin positive
B
CXCL2 mRNA levels (relative units)
Pre-reperfusion
Post-reperfusion
Murine LTX
C
C57Bl6
C57Bl6 Donor
Balb/C Recipient
Pre-ischemia
Post-ischemia 24h
BALF-TRAM
in vitro culture ±LPS +4hr
CXCL2 production
D
CXCL2 (pg/mL)
Pre-ischemia
Post-ischemia
Pre-ischemia+LPS
Post-ischemia+LPS

Figure 6

Figure 6. Ischemia-reperfusion primed TRAM have augmented response to endotoxin. (A) Relative *CXCL2* mRNA levels of human TRAM from endotoxin negative and positive patients pre- and post-reperfusion (n=6). (B) Fresh TRAM from endotoxin negative human donor lungs were isolated prior to transplantation or 120 min following reperfusion and then stimulated with endotoxin, *in vitro* (0.01 µg/mL LPS) (n=10). (C) Diagram depicting the experiments illustrated in (D) where TRAM harvested pre- and post-ischemia were challenged with LPS *in vitro.* (D) CXCL2 chemokine levels in the supernatant of murine TRAM harvested pre- and post-ischemia and challenged *in vitro* with LPS (0.01 µg/mL) for 4 h (n=3-4). (A), (B) and (C) graphs were analyzed by unpaired t-test. n.s. not significant; *p<0.05; **p<0.01; ****p<0.0001.

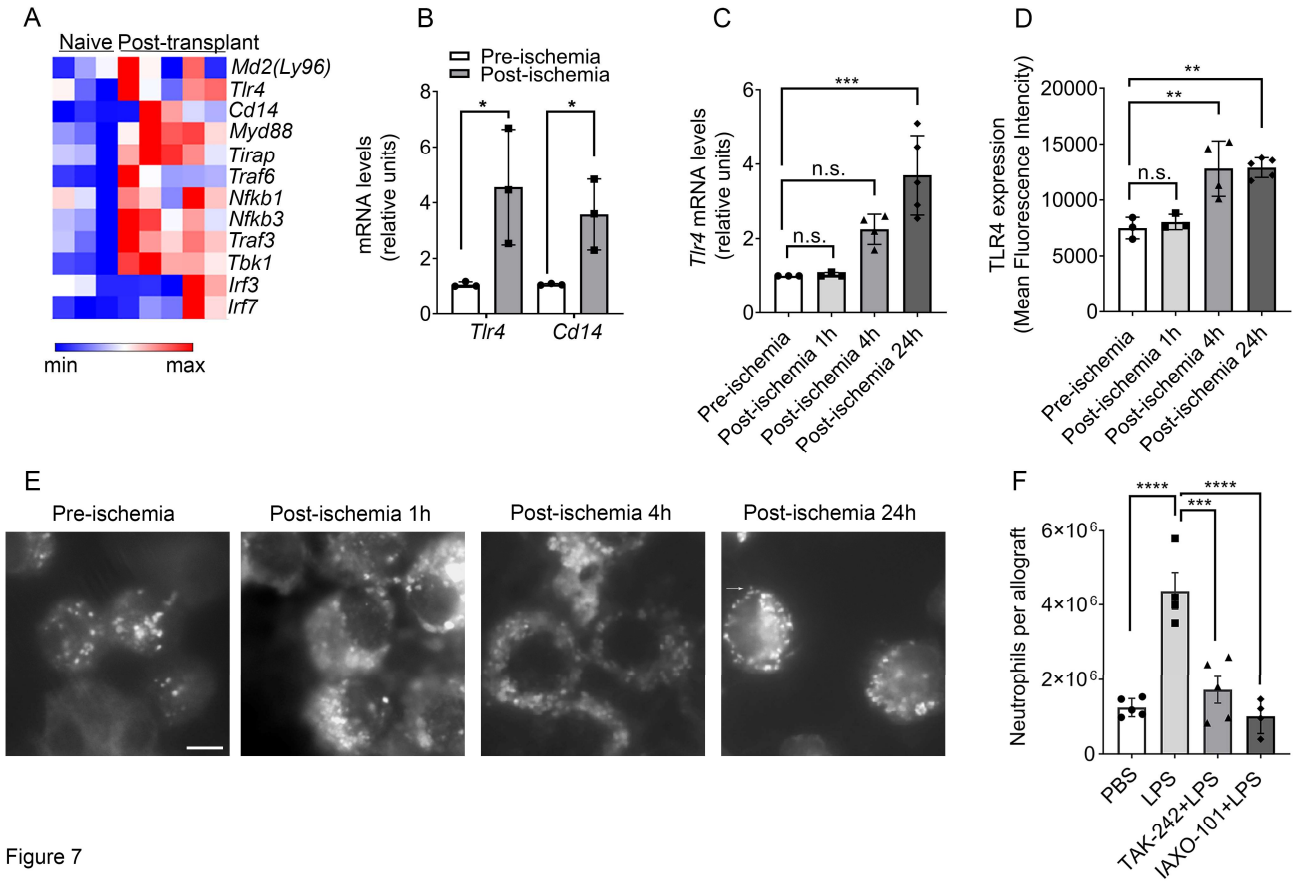
A
Naive Post-transplant
Md2(Ly96)
Tlr4
Cd14
Myd88
Tirap
Traf6
Nfkb1
Nfkb3
Traf3
Tbk1
Irf3
Irf7
min
max
B
Pre-ischemia
Post-ischemia
mRNA levels (relative units)
Tlr4
Cd14
C
Tlr4 mRNA levels (relative units)
n.s.
Pre-ischemia
Post-ischemia 1h
Post-ischemia 4h
Post-ischemia 24h
D
TLR4 expression (Mean Fluorescence Intencity)
n.s.
Pre-ischemia
Post-ischemia 1h
Post-ischemia 4h
Post-ischemia 24h
E
Pre-ischemia
Post-ischemia 1h
Post-ischemia 4h
Post-ischemia 24h
F
Neutrophils per allograft
PBS
LPS
TAK-242+LPS
IAXO-101+LPS

Figure 7

Figure 7. TRAM exposed to ischemia-reperfusion have increased TLR4 transcription and translocation to the plasma membrane. (A) Heatmap of selected TLR4 pathway genes expressed in murine donor TRAM exposed to ischemia-reperfusion (n=3-5). (B) *Tlr4* and *Cd14* mRNA expression in TRAM, harvested from BALF pre- and post-ischemia at 24h, was assessed by qPCR (n=3). (C) Expression level of *Tlr4* mRNA in TRAM harvested from BALF of pre-ischemia and 1h, 4h and 24h post-ischemia, assessed by qPCR (n=3-5). (D) Protein expression of TLR4 at the plasma membrane in TRAM harvested as in (C), assessed by flow cytometry (n=3-5). (E) Immunocytochemistry for TLR4 of TRAM harvested as described in (C). (F) Wild-type C57BL/6 donor mice were treated with low dose LPS-IT (0.5 µg/g BW) alone or in combination with TLR4 antagonist (TAK-242; 1 µg/g of BW, IV) or IAXO-101 (3 µg/g of BW, IT) and neutrophil recruitment was assessed 24h post-ischemia. Neutrophils were gated as live $CD45^{+}Ly6G^{+}CD11b^{+}CD24^{+}SSC^{hi}$ (n=4-5). (B) graph was analyzed by unpaired t-test. (C), (D) and (F) graphs were analyzed by one-way Anova followed by Tukey's post-hoc test. n.s. not significant; *p<0.05; **p<0.01; ***p<0.001; ****p<0.0001. Bar = 10 µm. Arrow points to TLR4 at the plasma membrane.

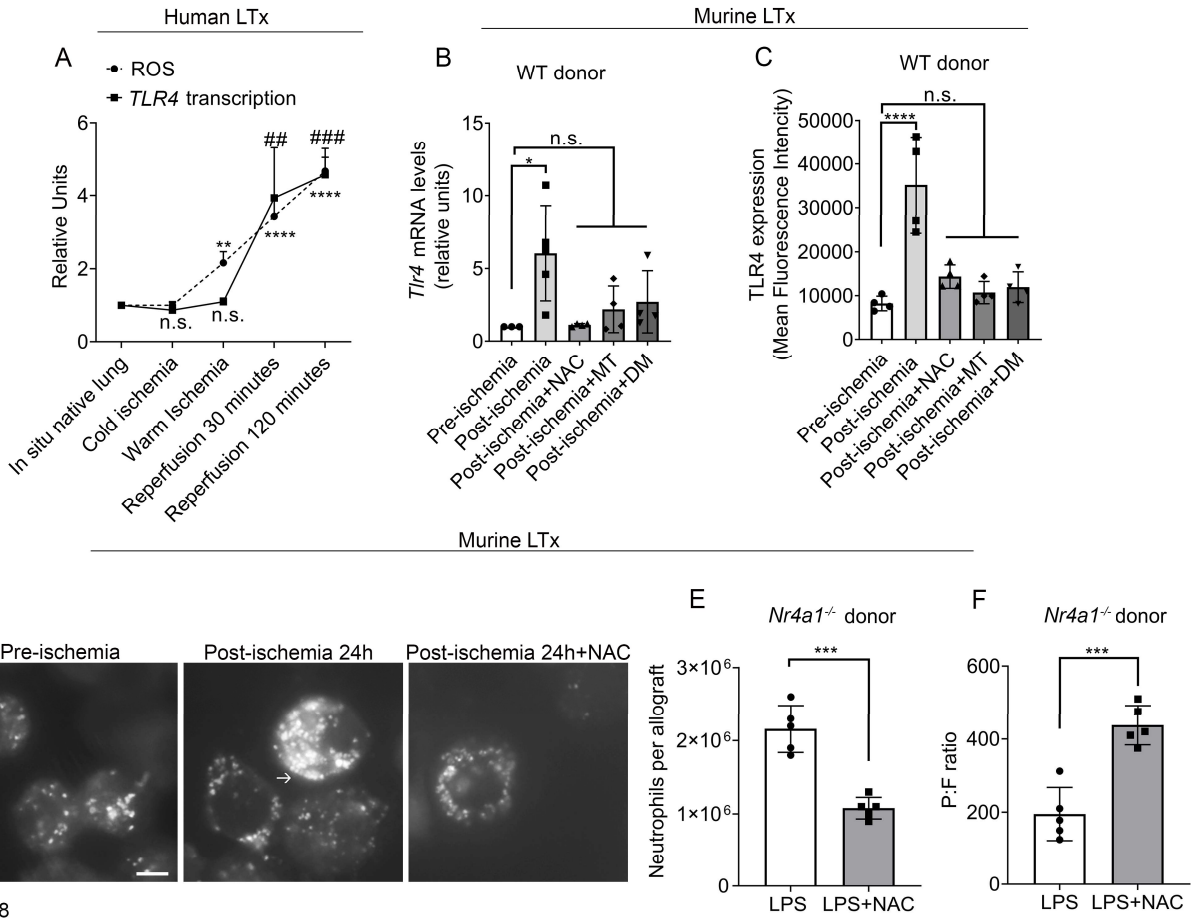
Human LTx
Murine LTx
A
ROS
TLR4 transcription
Relative Units
In situ native lung
Cold ischemia
Warm Ischemia
Reperfusion 30 minutes
Reperfusion 120 minutes
n.s.
n.s.
**
##
###
****
****
B
WT donor
Tlr4 mRNA levels (relative units)
n.s.
*
Pre-ischemia
Post-ischemia
Post-ischemia+NAC
Post-ischemia+MT
Post-ischemia+DM
C
WT donor
TLR4 expression (Mean Fluorescence Intencity)
n.s.
****
Murine LTx
D
Pre-ischemia
Post-ischemia 24h
Post-ischemia 24h+NAC
E
Nr4a1-/- donor
Neutrophils per allograft
***
LPS
LPS+NAC
F
Nr4a1-/- donor
P:F ratio
***
LPS
LPS+NAC

Figure 8

Figure 8. ROS produced during ischemia reperfusion are responsible for TLR4 up-regulation. (A) Human donor lungs being used for clinical transplantation were serially biopsied during the different phases of ischemia-reperfusion and development of reactive oxygen species (ROS) as well as *TLR4* transcription of flow-sorted donor TRAM determined. (B) WT Balb/c mice were transplanted with WT C57Bl/6 donor lungs. In order to test the effect of ROS on TLR4 expression in TRAM, we treated donors and recipient with N-acetyl-cysteine (NAC) (100 mg/kg BW), Mito-Tempo (MT) (5 mg/kg of BW, i.p) or Dimethyl malonate (DM) (10 mg/kg of BW, i.v), pre- and post-reperfusion. *Tlr4* mRNA levels were assessed 24 h post-ischemia by qPCR in TRAM harvested from BALF before and after transplantation (n=3-5). (C) Protein expression of TLR4 at the plasma membrane in TRAM harvested as in (B), assessed by flow cytometry (n=4). (D) Immunocytochemistry for TLR4 of TRAM harvested as described in (B). *Nr4a1*$^{-/-}$ donor lungs, which do not develop PGD, were administered low dose LPS and transplanted into WT recipients with or without NAC treatment. (E) Neutrophil infiltration was determined using flow-cytometry and (F) lung function using blood gases and P:F ratio. (B) and (C) graphs were analyzed by one-way Anova followed by Tukey's post-hoc test. (E) and (F) graphs were analyzed by unpaired t-test. n.s. not significant; *p<0.05; **p<0.01; ***p<0.001; ****p<0.0001. (A) * for ROS and # for TLR4 transcription. Bar = 10 µm. Arrow points to TLR4 at the plasma membrane.